

# TESTING CONDITIONAL INDEPENDENCE IN SUPERVISED LEARNING ALGORITHMS

BY DAVID S. WATSON<sup>\*,†</sup> AND MARVIN N. WRIGHT<sup>‡,§</sup>

*University of Oxford<sup>\*</sup>, The Alan Turing Institute<sup>†</sup>, Leibniz Institute for  
Prevention Research and Epidemiology<sup>‡</sup> and University of Copenhagen<sup>§</sup>*

We propose a general test of conditional independence. The conditional predictive impact (CPI) is a provably consistent and unbiased estimator of one or several features' association with a given outcome, conditional on a (potentially empty) reduced feature set. The measure can be calculated using any supervised learning algorithm and loss function. It relies on no parametric assumptions and applies equally well to continuous and categorical predictors and outcomes. The CPI can be efficiently computed for low- or high-dimensional data without any sparsity constraints. We illustrate PAC-Bayesian convergence rates for the CPI and develop statistical inference procedures for evaluating its magnitude, significance, and precision. These tests aid in feature and model selection, extending traditional frequentist and Bayesian techniques to general supervised learning tasks. The CPI may also be used in conjunction with causal discovery algorithms to identify underlying graph structures for multivariate systems. We test our method in conjunction with various algorithms, including linear regression, neural networks, random forests, and support vector machines. Empirical results show that the CPI compares favorably to alternative variable importance measures and other nonparametric tests of conditional independence on a diverse array of real and simulated datasets. Simulations confirm that our inference procedures successfully control Type I error and achieve nominal coverage probability. Our method has been implemented in an R package, `cpi`, which can be downloaded from <https://github.com/dswatson/cpi>.

**1. Introduction.** Variable importance (VI) is a major topic in statistics and machine learning. It is the basis of most if not all feature selection methods, which analysts use to identify key drivers of variation in an outcome of interest and/or create more parsimonious models. A large number of importance measures have been proposed in recent years, either for specific algorithms or more general applications. Several different notions of VI – some overlapping, some inconsistent – have emerged from this literature. We examine these in greater detail in Section 2.1.

One fundamental difference between various importance measures is whether they test the marginal or conditional independence of features. To evaluate response variable  $Y$ 's marginal dependence on predictor  $X_j$ , we

test against the following hypothesis:

Marginal:

$$H_0 : X_j \perp\!\!\!\perp Y, \mathbf{X}_{-j}$$

where  $\mathbf{X}_{-j}$  denotes a set of covariates. A measure of conditional dependence, on the other hand, tests against a different null hypothesis:

Conditional:

$$H_0 : X_j \perp\!\!\!\perp Y | \mathbf{X}_{-j}$$

Note that  $X_j$ 's marginal VI may be high due to its association with either  $Y$  or  $\mathbf{X}_{-j}$ . This is why measures of marginal importance tend to favor correlated predictors. Often, however, our goal is to determine whether  $X_j$  adds any new information to the model – in other words, whether  $Y$  is dependent on  $X_j$  even after conditioning on  $\mathbf{X}_{-j}$ . This becomes especially important when the assumption of feature independence is violated.

Tests of conditional independence (CI) are common in the causal modelling literature. For instance, the popular PC algorithm (Spirites, Glymour and Scheines, 2000), which infers a set of underlying directed acyclic graphs (DAGs) consistent with some observational data, relies on the results of CI tests to recursively remove the edges between nodes. Common parametric examples include the partial correlation test for continuous variables or the  $\chi^2$  test for categorical data. A growing body of literature in recent years has examined nonparametric alternatives to these options. We provide an overview of several such proposals in Section 2.2.

In this paper, we introduce a new CI test to measure VI. The conditional predictive impact (CPI) quantifies the contribution of one or several features to a given algorithm's predictive performance, conditional on some other (potentially empty) feature subset. It is an unbiased estimator that can be calculated using any supervised learner and loss function, and is provably consistent under minimal assumptions. We apply PAC-Bayesian convergence rates for the CPI and develop statistical inference procedures for evaluating its magnitude, precision, and significance. Finally, we demonstrate the measure's utility on a variety of real and simulated datasets.

The remainder of this paper is structured as follows. In Section 2, we review related work on VI measures and CI tests. We present theoretical results in Section 3, where we also outline an efficient algorithm for estimating the CPI, along with corresponding  $p$ -values and confidence intervals. We test our procedure on real and simulated data in Section 4, comparing its performance with popular alternatives under a variety of regression and

classification settings. Following a discussion in Section 5, we conclude in Section 6.

**2. Related Work.** In this section we survey the relevant literature on VI estimation and CI tests.

*2.1. Variable Importance Measures.* The notion of VI may feel fairly intuitive at first, but closer inspection reveals a number of underlying ambiguities. One important dichotomy is that between global and local measures, which respectively quantify the impact of features on all or particular predictions. This distinction has become especially important with the recent emergence of interpretable machine learning techniques designed to explain individual outputs of black box models (e.g., Datta, Sen and Zick, 2016; Lundberg and Lee, 2017; Ribeiro, Singh and Guestrin, 2016; Wachter, Mittelstadt and Russell, 2017). In what follows, we restrict our focus to global importance measures.

Another important dichotomy is that between model-specific and model-agnostic approaches. For instance, a number of methods have been proposed for estimating importance in linear regression (Barber and Candès, 2015; Grömping, 2007; Lindeman, Merenda and Gold, 1980), random forests (Breiman, 2001; Kursa and Rudnicki, 2010; Strobl et al., 2008), and neural networks (Bach et al., 2015; Gevrey, Dimopoulos and Lek, 2003; Shrikumar, Greenside and Kundaje, 2017). These measures have the luxury of leveraging an algorithm’s underlying assumptions and internal architecture for more precise and efficient VI estimation.

Other, more general techniques have also been developed. van der Laan (2006) derives efficient influence curves and inference procedures for a variety of VI measures. Hubbard, Kennedy and van der Laan (2018) build on this work, proposing a data-adaptive method for estimating the causal influence of variables within the targeted maximum likelihood framework (van der Laan and Rose, 2018). Williamson et al. (2017) describe an ANOVA-style decomposition of a regressor’s  $R^2$  into feature-wise contributions. Feng et al. (2018) design a neural network to efficiently compute this decomposition using multi-task learning. Candès et al. (2018) develop a probabilistic version of the “knockoff” procedure originally developed for linear models (Barber and Candès, 2015), extending the method to other learning algorithms. Fisher, Rudin and Dominici (2018) propose a number of “reliance” statistics, calculated by integrating a loss function over the empirical distribution of covariates while holding a given feature vector constant.

Perhaps the most important distinction between various competing notions of VI is the aforementioned split between marginal and conditional

measures. The topic has received considerable attention in the random forest literature, where Breiman’s popular permutation technique (2001) has been criticized for failing to properly account for correlations between features (Gregorutti, Michel and Saint-Pierre, 2015; Nicodemus et al., 2010). Conditional alternatives have been developed (Mentch and Hooker, 2016; Strobl et al., 2008), but we do not consider them here, as they are specific to tree ensembles.

Our proposed measure resembles what Fisher et al. 2018 call “algorithm reliance” (AR). The authors do not have much to say about AR in their paper, the majority of which is instead devoted to two related statistics they term “model reliance” (MR) and “model class reliance” (MCR). These measure the marginal importance of a feature subset in particular models or groups of models, respectively. Only AR measures the importance of the subset conditional on remaining covariates for a given supervised learner, which is our focus here. Fisher et al. derive probabilistic bounds for MR and MCR, but not AR. They do not develop hypothesis testing procedures for any of their reliance statistics.

*2.2. Conditional Independence Tests.* CI tests are the cornerstone of constraint-based and hybrid methods for causal graph inference and Bayesian network learning (Koller and Friedman, 2009; Korb and Nicholson, 2009; Scutari and Denis, 2014). Assuming the causal Markov condition and faithfulness – which together state (roughly) that statistical independence implies graphical independence and vice versa – a number of algorithms have been developed that use CI tests to discover an equivalence class of DAGs consistent with a set of observational data (Maathuis, Kalisch and Bühlmann, 2009; Verma and Pearl, 1991; Spirtes, Glymour and Scheines, 2000).

Shah and Peters (2018) have shown that there exists no uniformly valid CI test. Parametric assumptions are typically deployed to restrict the range of alternative hypotheses, which is default behavior for most causal discovery software (e.g., Kalisch et al., 2012; Scutari, 2010). However, more flexible methods have been introduced. Much of this literature relies on techniques that embed the data in a reproducing kernel Hilbert space (RKHS). For instance, Fukumizu et al. (2008) use a normalized cross-variance operator to test the association between features in the RKHS. A null distribution is approximated via permutation. Doran et al. (2014) build on Fukumizu et al.’s work with a modified permutation scheme intended to capture the effects of CI. Zhang et al. (2012) derive a test statistic from the traces of kernel matrices, using a gamma null distribution to compute statistical significance.

Because kernel methods do not scale well with sample size, several authors have proposed more efficient alternatives. For instance, [Strobl, Zhang and Visweswaran \(2017\)](#) employ a fast Fourier transform to reduce the complexity of matrix operations. Methods have been developed for estimating regularized, nonlinear partial correlations ([Ramsey, 2014](#); [Shah and Peters, 2018](#)). [Chalupka, Perona and Eberhardt \(2018\)](#) propose a kind of modified likelihood ratio test (LRT) in which decision trees are grown on data with and without the variable(s) of interest. The predictive performance of full and reduced models is compared to evaluate the conditional importance of the dropped feature(s).

Our proposal is conceptually similar to the LRT-inspired approach of Chalupka et al. However, there are theoretical issues with their procedure. First, as Fisher et al. [2018](#) point out, algorithms that require a minimum number of features may not be well-defined upon deletion of a feature subset. More importantly, the statistical test that Chalupka et al. outline does not follow the purported null distribution for arbitrary input algorithms.

For example, the addition of new covariates can never hurt the in-sample performance of a linear model. That is why the log-ratio of nested model likelihoods is strictly positive, proportional to a  $\chi^2$ -distribution under the null hypothesis of the classical LRT, which is calculated on in-sample risk ([Wilks, 1938](#)). By contrast, the addition of uninformative covariates will tend to hurt a linear model’s performance on unseen data. Using out-of-sample likelihoods, log-ratios under the null hypothesis are centered around some negative number, with a long right tail. Under either mode of evaluation, using in-sample or out-of-sample risk, null results do not generally follow the  $t$ -distribution that Chalupka et al. advocate. However, the  $t$ -test can be applied under a different model refitting and evaluation procedure, as described in [Section 3.2](#).

**3. Theory.** The basic intuition behind our approach is that important features should be *informative* – that is, their inclusion should improve the predictive performance of an appropriate algorithm as measured by some preselected loss function. Moreover, the significance of improvement should be quantifiable so that error rates can be controlled at user-specified levels.

Allow us to spell this out more precisely. Consider an  $n \times p$  feature matrix  $\mathbf{X} \in \mathcal{X}$  and corresponding response variable  $Y \in \mathcal{Y}$ , which combine to form the dataset  $\mathbf{Z} = (\mathbf{X}, Y) \in \mathcal{Z}$ . Each observation  $\mathbf{z}_i = (\mathbf{x}_i, y_i)$  is an i.i.d. sample from a fixed but unknown joint probability distribution,  $\mathbb{P}(\mathbf{Z}) = \mathbb{P}(\mathbf{X}, Y)$ . Let  $\mathbf{X}^S \subseteq (X_1, \dots, X_p)$  denote some subset of the feature space whose predictive impact we intend to quantify, conditional on the (possibly

empty) set of remaining covariates  $\mathbf{X}^R = \mathbf{X} \setminus \mathbf{X}^S$ . Data can now be expressed as a triple,  $\mathbf{Z} = (\mathbf{X}^S, \mathbf{X}^R, Y)$ . We remove the predictive information in  $\mathbf{X}^S$  by performing a single random permutation on its rows, rendering a new dataset,  $\tilde{\mathbf{Z}} = (\tilde{\mathbf{X}}^S, \mathbf{X}^R, Y)$ , where the tilde denotes permutation.

Define a function  $f \in \mathcal{F}, \mathcal{F} : \mathcal{X} \rightarrow \mathcal{Y}$  as a mapping from features to outcomes, and an algorithm  $a \in \mathcal{A}, \mathcal{A} : \mathcal{Z} \rightarrow \mathcal{F}$  as a mapping from datasets to functions. Consider a function space  $\mathcal{F}_a$  in the range of  $a$ , and let  $\{f, f_0\} \in \mathcal{F}_a$  denote original and null models trained on  $\mathbf{Z}$  and  $\tilde{\mathbf{Z}}$ , respectively. We assume that all functions in  $\mathcal{F}_a$  share the same architecture and hyperparameters. For instance, if  $a$  is a neural network, then models may differ in their weights and biases but not in their number of layers and nodes. We evaluate a model's performance using some real-valued, nonnegative loss function  $L$ . Define the risk of  $f$  with respect to  $\mathbf{Z}$  as its expected loss over the joint probability distribution  $\mathbb{P}(\mathbf{Z})$ ,  $R(f, \mathbf{Z}) = \mathbb{E}[L(f, \mathbf{Z})]$ . Our strategy is to replace the conditional null hypothesis defined in Section 1 with the following:

Conditional Predictive:

$$H_0 : R(f, \mathbf{Z}) \geq R(f_0, \tilde{\mathbf{Z}})$$

In other words, we test whether the risk of the original model trained on the observed data is at least as great as that of the null model trained on the permuted data.

**3.1. Consistency and Convergence.** The CPI of submatrix  $\mathbf{X}^S$  measures the extent to which the feature subset improves predictions made using algorithm  $a$ . These improvements may be additive or multiplicative, depending on a variety of factors. We therefore propose two closely related measures – one based on risk differences, the other on risk ratios – and introduce estimation procedures for both.

Assume that the loss function  $L$  can be evaluated for each sample  $i$ .<sup>1</sup> We may then define the following two random variables:

$$\Delta_i = L(f_0, \tilde{\mathbf{z}}_i) - L(f, \mathbf{z}_i) \tag{1}$$

$$\lambda_i = \log \left( \frac{L(f_0, \tilde{\mathbf{z}}_i)}{L(f, \mathbf{z}_i)} \right) \tag{2}$$

These represent the difference and log-ratio, respectively, of sample-wise loss between null and original models. We define additive and multiplicative

---

<sup>1</sup>For loss functions that do not have this property, such as the area under the receiver operating characteristic curve, the following arguments can easily be modified to apply to each fold in a cross-validation, rather than each sample in a dataset.

forms of CPI by taking the expectation of each:

$$\text{CPI}_\Delta(\mathbf{X}^S) = \mathbb{E}[\Delta] \quad (3)$$

$$\text{CPI}_\lambda(\mathbf{X}^S) = \mathbb{E}[\lambda] \quad (4)$$

Note that the CPI is always a function of some feature subset  $\mathbf{X}^S$ . We omit the parenthetical for notational convenience moving forward.

To consistently estimate either statistic, it is necessary and sufficient to show that we can consistently estimate loss for models in  $\mathcal{F}_a$ . The population parameter  $R(f, \mathbf{Z})$  is estimated using the empirical risk formula:

$$R_{\text{emp}}(f, \mathbf{Z}) = \frac{1}{m} \sum_{i=1}^m L(f, \mathbf{z}_i) \quad (5)$$

Our goal in estimating risk is to evaluate how well a model generalizes beyond its training data, so the  $m$  samples in Eq. 5 constitute a test set drawn independently from  $\mathbf{Z}$ , distinct from the  $n$  samples used to fit  $f$ . In practice, this is typically achieved by some resampling procedure like cross-validation or bootstrapping. In what follows, we presume that unit-level loss  $L(f, \mathbf{z}_i)$  is always an out-of-sample evaluation, such that  $f$  was trained on data excluding  $\mathbf{z}_i$ .

The empirical risk minimization (ERM) principle is a simple decision procedure in which we select the function  $f$  that minimizes empirical risk in some function space  $\mathcal{F}$ . A celebrated result of [Vapnik and Chervonenkis \(1971\)](#), independently derived by [Sauer \(1972\)](#) and [Shelah \(1972\)](#), is that the ERM principle is consistent with respect to  $\mathcal{F}$  if and only if the function space is of finite VC dimension. Thus for any algorithm that meets this minimal criterion, the empirical risk  $R_{\text{emp}}(f, \mathbf{Z})$  converges uniformly in probability to  $R(f, \mathbf{Z})$  as  $n \rightarrow \infty$ , which means the estimates

$$\widehat{\text{CPI}}_\Delta = \frac{1}{n} \sum_{i=1}^n L(f_0, \tilde{\mathbf{z}}_i) - L(f, \mathbf{z}_i) \quad (6)$$

and

$$\widehat{\text{CPI}}_\lambda = \frac{1}{n} \sum_{i=1}^n \log \left( \frac{L(f_0, \tilde{\mathbf{z}}_i)}{L(f, \mathbf{z}_i)} \right) \quad (7)$$

will likewise converge to their true values at a rate equal to the minimum convergence rate of  $\{f, f_0\}$ , provided  $R(f, \mathbf{Z}) > 0$ .

These rates may be calculated using the standard tools of statistical learning theory ([Valiant, 1984](#); [Vapnik, 1998](#)), which typically derive probabilistic

bounds as functions of VC dimension or some other capacity measure. Unfortunately, capacity can be difficult to compute for complex algorithms. Another alternative, better suited to the present case, is to place a prior probability on the function class  $\mathcal{F}_a$  corresponding to each model's chance of converging first. This enables a Probably Approximately Correct (PAC)-Bayesian analysis, which provides tighter, more informative bounds than those based on capacity measures.

Let  $\pi(f_0)$  denote the prior probability that  $R_{\text{emp}}(f_0, \tilde{\mathbf{Z}})$  converges to  $R(f_0, \tilde{\mathbf{Z}})$  faster than  $R_{\text{emp}}(f, \mathbf{Z})$  converges to  $R(f, \mathbf{Z})$ . There is no reason to believe that this value should be greater than its complement,  $\pi(f) = 1 - \pi(f_0)$ , given that  $\mathbb{P}(\tilde{\mathbf{Z}})$  is a random perturbation of the true underlying joint distribution  $\mathbb{P}(\mathbf{Z})$ . Then the simplest PAC-Bayesian bound for  $f_0$ , assuming binomial loss  $L \in \{0, 1\}$ , is found in Eq. 8. With probability at least  $1 - \delta$ :

$$R(f_0, \tilde{\mathbf{Z}}) \leq R_{\text{emp}}(f_0, \tilde{\mathbf{Z}}) + \sqrt{\frac{\log(1/\pi(f_0)) + \log(1/\delta)}{2n}} \quad (8)$$

This formula, like all PAC-Bayesian bounds, expresses the convergence rate as a function of a prior probability, as opposed to a potentially elusive capacity measure. PAC-Bayesian rates hold uniformly for any valid prior distribution, which means we may choose for concreteness, and without loss of generality, a default of  $\pi(f_0) = \pi(f) = 0.5$ , although this almost certainly overestimates  $\pi(f_0)$ . In any event, PAC-Bayesian methods provide tighter bounds than classical statistical learning theory, which has tended to focus on worst-case convergence rates that place undue emphasis on degenerate functions or joint distributions. Many PAC-Bayesian bounds have been derived, including extensions to unbounded loss functions for classification and regression. For an overview, see (Germain et al., 2016).

Because the log-ratio  $\log(x/y)$  is equivalent to the difference  $\log(x) - \log(y)$ , inference procedures for either CPI measure can be designed using any paired difference test. Familiar frequentist examples include the  $t$ -test and the Fisher exact test, which we use for large- and small-sample settings, respectively.

Bayesian analogues can easily be implemented as well. Rouder et al. (2009) advocate an analytic strategy for calculating Bayes factors for  $t$ -tests. Wetzel et al. (2009) and Kruschke (2013) propose more general methods based on Markov chain Monte Carlo sampling, although they differ in their proposed priors and decision procedures. Care should be taken when selecting a prior distribution in the Bayesian setting, especially with small sample sizes. Tools for Bayesian inference are implemented in the `cpi` package; however,



for brevity's sake, we restrict the following sections to frequentist methods.

**3.2. Large Sample Inference: Paired  $t$ -tests.** By the central limit theorem, empirical risk estimates for functions of finite VC dimension will tend to be normally distributed around the true population parameter value. This suggests that the significance of CPI measures may be evaluated using paired, one-sided  $t$ -tests. However, we have found convergence rates for risk differences to be prohibitively slow. Log-ratios, on the other hand, do follow the purported null distribution in large samples, leading to better Type I error control. This conclusion is corroborated by extensive simulation experiments in Section 4.1.

The variable  $\lambda$  has mean  $\widehat{\text{CPI}}_\lambda$  and standard error  $\text{SE} = \hat{\sigma}/\sqrt{n}$ , where  $\hat{\sigma} = [\sum_{i=1}^n (\lambda_i - \widehat{\text{CPI}}_\lambda)^2 / (n-1)]^{1/2}$ . The  $t$ -score for  $\widehat{\text{CPI}}_\lambda$  is given by  $t = \widehat{\text{CPI}}_\lambda / \text{SE}$ , and we compute  $p$ -values by comparing this statistic to the most tolerant distribution consistent with  $H_0 : R(f, \mathbf{Z}) \geq R(f_0, \tilde{\mathbf{Z}})$ , namely  $t_{n-1}$ . To control Type I error at level  $\alpha$ , we reject  $H_0$  for all  $t$  greater than or equal to the  $(1 - \alpha)$  quantile of  $t_{n-1}$ . This procedure can easily be modified to adjust for multiple testing.

Predictive variance can optionally be incorporated into the test if reliable estimates are available. Simply record precision weights for each prediction equal to the inverse of its variance. Then use these values to fit a weighted least squares regression with a  $2n \times (n+1)$  feature matrix – with coefficients for each unit  $i = \{1, \dots, n\}$ , as well as an indicator variable for model type  $W$  (original vs. null) – to predict expected log-transformed loss. The  $t$ -statistic and  $p$ -value associated with coefficient  $\beta_W$  can be computed from these outputs as outlined above.

Confidence intervals around  $\widehat{\text{CPI}}_\lambda$  may be constructed in the typical manner. The lower bound is set by subtracting from our point estimate the product of SE and  $F_{n-1}^{-1}(1 - \alpha)$ , where  $F_{n-1}(\cdot)$  denotes the CDF of  $t_{n-1}$ . Using this formula, we obtain a 95% confidence interval for  $\widehat{\text{CPI}}_\lambda$  by calculating  $[\widehat{\text{CPI}}_\lambda - \text{SE} \times F_{n-1}^{-1}(0.95), \infty)$ . As  $n$  grows large, this interval converges to the Wald-Type Interval,  $[\widehat{\text{CPI}}_\lambda - \text{SE} \times \Phi^{-1}(0.95), \infty)$ , where  $\Phi$  represents the standard normal CDF.

**3.3. Small Sample Inference: Fisher Exact Tests.** Paired  $t$ -tests will tend to have low sensitivity and specificity with small sample sizes. In such cases, exact  $p$ -values may be computed for a slightly modified null hypothesis using Fisher's method (1935), a nonparametric technique that works equally well with risk differences and ratios. Rather than focusing on overall risk, this null hypothesis states that permuting the rows of  $\mathbf{X}^S$  has no effect on unit-level

loss. More formally, we test against the following:

$$H_0^{\text{FEP}} : L(f, \mathbf{z}_i) \geq L(f_0, \tilde{\mathbf{z}}_i), i = 1, \dots, n.$$

Under this null hypothesis, which is sufficient but unnecessary for the conditional predictive  $H_0$ , we may implement a permutation scheme in which the CPI is calculated for all possible assignments of model type  $W$ . Consider a  $2n \times 3$  matrix with columns for unit index  $U = \{1, 1, \dots, n, n\}$ , assignment  $W \in \{0, 1\}$ , and loss  $L$ . We permute the rows of  $W$  subject to the constraint that every sample's loss is recorded under both original and null models. For each possible assignment vector  $W$ , compute the resulting CPI (using either  $\lambda$  or  $\Delta$  vectors) and compare the value of our observed statistic,  $\widehat{\text{CPI}}$ , to the complete distribution. Note that this paired setup dramatically diminishes the possible assignment space from an unmanageable  $\binom{2n}{n}$ , corresponding to a Bernoulli trial design, to a more reasonable  $2^n$ . The one-tailed Fisher exact  $p$ -value (FEP) is given by the formula:

$$\text{FEP}(\widehat{\text{CPI}}) = \frac{1}{2^n} \sum_{b=1}^{2^n} \mathbf{1}_{\widetilde{\text{CPI}}_b \geq \widehat{\text{CPI}}}$$

where  $\mathbf{1}$  represents the indicator function and  $\widetilde{\text{CPI}}_b$  is the CPI resulting from the  $b^{\text{th}}$  permutation of  $W$ .

To construct a confidence interval for  $\widehat{\text{CPI}}$  at level  $1 - \alpha$ , we use our empirical null distribution. Find the critical value  $\text{CPI}^*$  such that  $\text{FEP}(\text{CPI}^*) = \alpha$  and calculate the difference  $\delta = \text{CPI}^* - \widehat{\text{CPI}}$ . Then a  $(1 - \alpha) \times 100\%$  confidence interval for  $\widehat{\text{CPI}}$  is given by  $[\widehat{\text{CPI}} - \delta, \infty)$ . For  $n$  large, approximate calculations can be made by sampling from the set of  $2^n$  permissible permutations. In this case, however, it is important to add 1 to both the numerator and denominator to ensure unbiased inference and avoid  $p$ -values of 0 ([Phipson and Smyth, 2010](#)).

**3.4. Computational Complexity.** To summarize, we outline our proposed algorithm for testing the conditional importance of feature subsets for su-

pervised learners in pseudocode below.

---

**Algorithm 1:** CPI Algorithm

---

- Input:** Dataset  $\mathbf{Z}$ , submatrix  $\mathbf{X}^S$ , supervised learner  $a$ , risk functional  $R$ , risk estimator  $k$ , CPI measure  $m$ , inference procedure  $h$
1. Permute the rows of  $\mathbf{X}^S$  to create new dataset  $\tilde{\mathbf{Z}}$
  2. Train  $a$  on  $\mathbf{Z}$  and  $\tilde{\mathbf{Z}}$  to create models  $f$  and  $f_0$ , respectively
  3. Use risk estimator  $k$  to compute each  $L(f, \mathbf{z}_i)$  and  $L(f_0, \tilde{\mathbf{z}}_i)$
  4. Calculate  $\widehat{\text{CPI}}$  with measure  $m$
  5. Apply inference procedure  $h$  to determine associated  $p$ -value ( $p$ ) and confidence interval (ci)

**Output:**  $\widehat{\text{CPI}}$ ,  $p$ , ci

---

This algorithm executes in  $\mathcal{O}(ak + h)$  time. In other words, computational complexity is wholly determined by three factors: the learner  $a$ , the empirical risk estimator  $k$ , and the inference test  $h$ . We take the complexity of  $a$  to be given. The empirical risk estimator  $k$  can be made more or less complex depending on the resampling procedure. The most efficient option for evaluating generalization error is the holdout method, in which a model is trained on a random subset of the available data and tested on the remainder. Unfortunately, this procedure can be unreliable with small sample sizes. Popular alternatives include the bootstrap and cross-validation. Both require considerable model refitting, which can be costly when  $a$  is complex.

The inference procedure  $h$  is quite efficient in the parametric case – on the order of  $\mathcal{O}(n)$  for the  $t$ -test – but scales exponentially with the sample size when using the permutation-based approach. As noted above, the complexity of the Fisher test can be bounded by setting an upper limit on the number of permutations  $B$  used to approximate the empirical null distribution. The standard error of a  $p$ -value estimate made using such an approximation is  $\sqrt{p^*(1 - p^*)/B}$ , where  $p^*$  represents the true  $p$ -value. This expression is maximized at  $p^* = 0.5$ , corresponding to a standard error of  $1/(2\sqrt{B})$ . Thus, to guarantee a standard error of at most 0.001, it would suffice to use  $B = 250,000$  permutations, an eminently feasible computation using parallel processors.

**4. Experiments.** All experiments were conducted in the R statistical computing environment, version 3.5.1. Code for reproducing all results and figures can be found in our dedicated GitHub repository: [https://github.com/dswatson/cpi\\_paper](https://github.com/dswatson/cpi_paper).

4.1. *Simulated Data.* We report results from a number of simulation studies. First, we analyze the statistical properties of our proposed tests under null and alternative hypotheses. We proceed to compare the sensitivity and specificity of the CPI to those of several alternative measures.

Data were simulated under two scenarios. In the linear scenario, ten uniformly distributed variables  $\mathbf{X} = X_1, \dots, X_{10}$  were generated and a continuous outcome  $Y$  was calculated as  $Y = \mathbf{X}\boldsymbol{\beta} + \epsilon$ , where  $\boldsymbol{\beta} = (0, 0, -0.5, 0.5, -1, 1, -1.5, 1.5, -2, 2)^\top$  and  $\epsilon \sim \mathcal{N}(0, 1)$ . In the nonlinear scenario, we keep the same predictors but generate the response from a transformed matrix,  $Y = \mathbf{X}^*\boldsymbol{\beta} + \epsilon$ , where

$$x_{ij}^* = \begin{cases} 1, & \text{if } 0.25 \leq x_{ij} \leq 0.75 \\ 0, & \text{else} \end{cases}$$

with the same  $\boldsymbol{\beta}$  and  $\epsilon$  as in the linear case. A similar simulation was performed for a classification outcome, where the response  $Y$  was drawn from a binomial distribution with probability  $[1 + \exp(-\mathbf{X}\boldsymbol{\beta})]^{-1}$  and  $[1 + \exp(-\mathbf{X}^*\boldsymbol{\beta})]^{-1}$  for the linear and nonlinear case, respectively.

4.1.1. *Type I and Type II Errors.* We simulate 10,000 datasets with  $n = 1,000$  observations and compute the CPI using four different learning algorithms: linear/logistic regression (LM), random forests (RF), artificial neural network (ANN), and support vector machine (SVM). Risk was estimated using 5-fold cross validation. For regression models, we used mean square error (MSE) and mean absolute error (MAE) loss functions; for classification, we used cross entropy (CE) and mean misclassification error (MMCE). We computed  $p$ -values via the inference procedures described in Section 3, i.e. paired  $t$ -tests and Fisher exact tests. For Fisher tests we used 10,000 permutations.

Linear and logistic regressions were built using the functions `lm()` and `glm()`, respectively, from the R package `stats` (R Core Team, 2018). RFs were built using the `ranger` package (Wright and Ziegler, 2017), with 50 trees. ANNs were built with the `nnet` package (Venables and Ripley, 2002), with 20 hidden units and a weight decay of 0.1. SVMs were built with the `e1071` package (Meyer et al., 2018), using a Gaussian radial basis function (RBF) kernel and  $\sigma = 1$ . Unless stated otherwise, all hyperparameters were left to their default values. Cross-validation was performed with the `mlr` package (Bischl et al., 2016).

Significance levels for all tests were fixed at  $\alpha = 0.05$ . For each simulation, we calculated the CPI values, Type I errors, Type II errors, empirical coverage, and  $t$ -statistics, where applicable. Results for MSE loss are shown

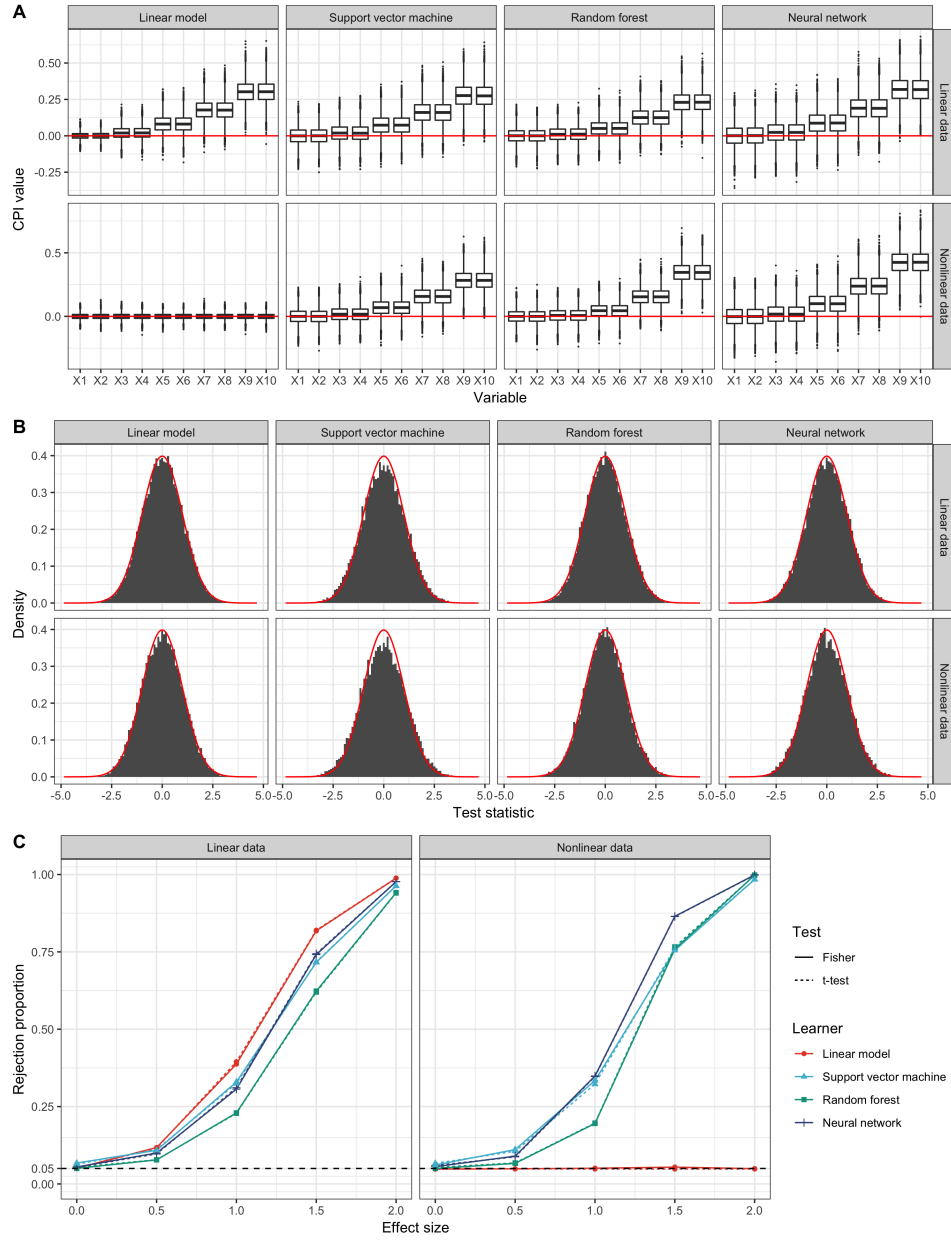


FIG 1. Simulation results for continuous outcome with MSE loss and multiplicative CPI. **A:** Boxplots of simulated CPI values of variables  $X_1, \dots, X_{10}$  with increasing effect size. The red line indicates a CPI value of 0, corresponding to a completely uninformative predictor  $X_j$ . **B:** Histograms of simulation replications of t-statistics of variables with effect size 0. The distribution of the expected t-statistic under the null hypothesis is shown in red. **C:** Proportion of rejected hypotheses at  $\alpha = 0.05$  as a function of effect size. Results at effect size 0 correspond to the Type I error, at effect sizes  $> 0$  to statistical power. The dashed line indicates the nominal level of  $\alpha = 0.05$ . The panels correspond to the simulation scenario, the colors and symbols to the learning algorithms, and the line types to the inference procedure.

in Fig. 1. Similar plots for MAE, CE, and MMCE loss functions are presented in Figs. S1-S8 of the supplement. Coverage probabilities are shown in Tables S1-S8 of the supplement.

For continuous outcomes,  $\text{CPI}_\lambda$  controlled Type I error with all four learners and reached 80% power at an effect size of 2.0, except for the LM, which, as expected, had no power in the nonlinear data. We observed no difference between the MSE and MAE loss functions.  $\text{CPI}_\Delta$  proved more sensitive than  $\text{CPI}_\lambda$ , but at the cost of slightly inflated Type I error rates with all learners except the LM. Again, we observed no difference between the MSE and MAE loss functions.

For categorical outcomes, both  $\text{CPI}_\lambda$  and  $\text{CPI}_\Delta$  controlled Type I error for the MMCE loss with all four learners. However, 80% power at an effect size of 2.0 was only achieved on the nonlinear data. With CE loss,  $\text{CPI}_\lambda$  showed inflated Type I errors with all four learners, peaking at  $\alpha = 0.25$  for the SVM. The  $\text{CPI}_\Delta$  controlled Type I error with LM and RF, but failed to do so with the SVM and ANN. The reason for this might be that CE is calculated based on predicted probabilities, which are known to be poorly calibrated for SVMs (Niculescu-Mizil and Caruana, 2005) and ANNs (Guo et al., 2017). Statistical power was generally greater with CE loss than with MMCE loss.

**4.1.2. Comparative Performance.** We use the same simulation setup to compare the CPI’s performance to that of three other global, nonparametric, model-agnostic measures of CI:

- **ANOVA:** Williamson et al. (2017)’s nonparametric ANOVA-inspired VI, as implemented in the R package `vimp`, version 1.1.4.
- **FCIT:** A modified version of Chalupka, Perona and Eberhardt (2018)’s fast conditional independence test, where decision trees are replaced by the supervised learners specified above. Differences in loss are calculated by sample instead of by cross-validation fold.
- **GCM:** Shah and Peters (2018)’s generalized covariance measure, a nonparametric estimate of the partial correlation between two vectors.

Unfortunately, software for Hubbard, Kennedy and van der Laan (2018) targeted maximum likelihood VI statistic was still under development at the time of testing, and beta versions generated errors. Candès et al.’s probabilistic knockoff procedure (2018) can be extended to nonparametric models, but requires an algorithm-specific VI measure, which not all learners provide. Kernel methods do not work with arbitrary algorithms and were therefore excluded as incomparable. We restrict this section to the regression setting, as only FCIT can be extended to classification problems.

We kept the train/test ratio constant at 2:1 and varied the training sample size from  $n = 100$  to  $n = 500$  and  $n = 1,000$ . For each training sample, we fit LM, RF, ANN, and SVM regressions, as described in Section 4.1.1. For each model, we estimated the VI of all features on the test set. This procedure was repeated 10,000 times. Results for  $n = 1,000$  are plotted in Fig. 2. Results for smaller sample sizes are included in the supplement. An ideal CI test would have a 5% rejection rate under the null hypothesis of effect size = 0 and a 100% rejection rate for all nonzero effect sizes.

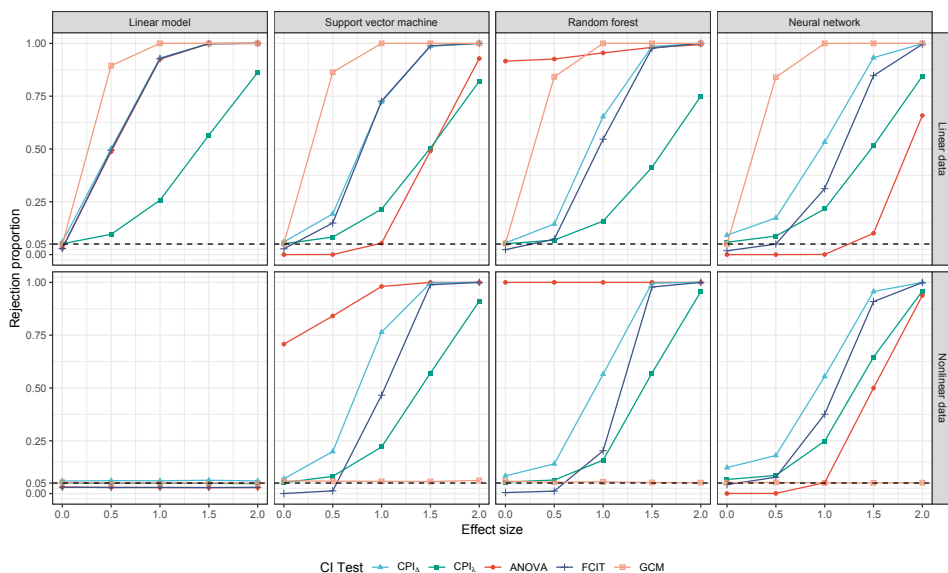


FIG 2. *Comparative performance of VI measures across different simulations and algorithms. Plots depict the proportion of rejected hypotheses at  $\alpha = 0.05$  as a function of effect size. Results at effect size 0 correspond to Type I error, at effect sizes  $> 0$  to statistical power. The dashed line indicates the nominal level of  $\alpha = 0.05$ . These results were computed using a training sample of  $n = 1,000$  and a test sample of  $n = 500$ . Similar results were obtained for train/test splits of  $n = 100/50$  and  $n = 500/250$  (see Supplementary Materials).*

All methods have high Type II error rates when fitting an LM to nonlinear data, highlighting the dangers of model misspecification. GCM appears to dominate for linear data, but struggles to detect VI in nonlinear simulations. The nonparametric ANOVA generally performs poorly, especially with RF regressions, where we observed Type I error rates north of 80%. FCIT is somewhat conservative, often falling well short of the nominal Type I error under the null hypothesis. The method improves as effect size grows,

although it is typically less sensitive than  $\text{CPI}_\Delta$ .

As observed in Section 4.1.1,  $\text{CPI}_\Delta$  generally has greater statistical power than  $\text{CPI}_\lambda$ , although the latter is better able to control Type I error. In fact, the only methods that control Type I error under all combinations in the grid are GCM and  $\text{CPI}_\lambda$ . The latter does so with greater power than the former in nonlinear simulations, while the relationship is reversed for linear data.

4.2. *Real Data.* In this section, we apply the CPI to real datasets of low- and high-dimensionality.

4.2.1. *Boston Housing.* We analyzed the Boston housing data (Harrison and Rubinfeld, 1978), which consists of 506 observations and 14 variables. This benchmark dataset is available in the UCI Machine Learning Repository (Dua and Taniskidou, 2017). The dependent variable is the median price of owner-occupied houses in census tracts in the Boston metropolitan area in 1970. The independent variables include the average number of rooms, crime rates, and air pollution.

Using LM and SVM regressions, we computed  $\text{CPI}_\lambda$ , standard errors, and  $t$ -test  $p$ -values for each feature, adjusting for multiple testing using Holm’s (1979) procedure. We used an RBF kernel for the SVM, measured performance via MSE, and used 20 subsampling iterations to evaluate empirical risk. The results are shown in Fig. 3. We found significant effects at  $\alpha = 0.05$  for the average number of rooms (`rm`), pupil-teacher ratio (`ptratio`), percentage of lower status of the population (`lstat`), distance to employment centers (`dis`), and the proportion of blacks (`b`) with both LM and SVM, which is in line with previous analyses (Friedman and Popescu, 2008; Williamson et al., 2017). Interestingly, the SVM assigned a higher  $\text{CPI}_\lambda$  value to several variables compared to the LM. For example, the proportion of owner-occupied units built prior to 1940 (`age`) significantly increased the predictive performance of the SVM but had approximately zero impact on the LM. The reason for this difference might be a nonlinear interaction between `rm` and `age`, which was also observed by Friedman and Popescu (2008).

4.2.2. *Breast Cancer.* We examined gene expression profiles of human breast cancer samples downloaded from GEO series GSE3165. Only the 94 arrays of platform GPL887 (Agilent Human 1A Microarray V2) were included. These data were originally analyzed by Herschkowitz et al. (2007) and later studied by Lim et al. (2009). We follow their preprocessing pipeline, leaving 13,064 genes. All samples were taken from tumor tissue and classified



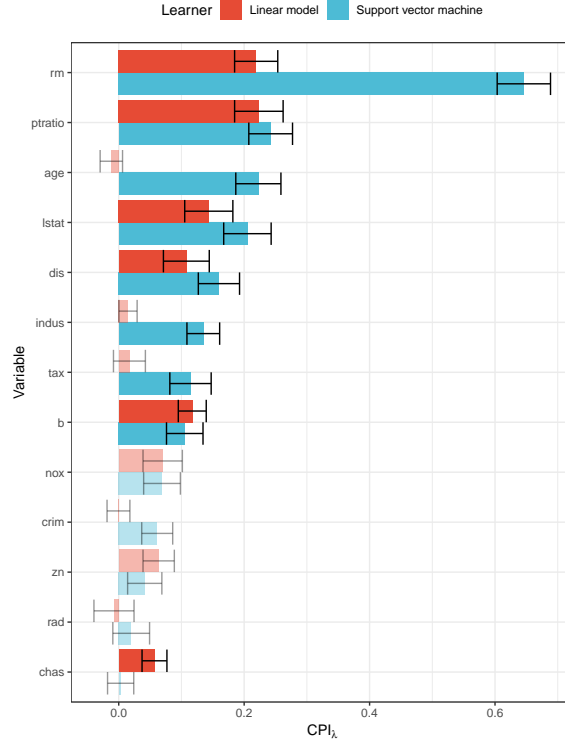


FIG 3. Results of the Boston housing experiment. For each variable in the data set, the  $CPI_k$  value is shown, computed with a linear model and a support vector machine. Whiskers represent standard errors. Non-significant variables at  $\alpha = 0.05$  after adjustment for multiple testing are shaded.

into one of six molecular subtypes: basal-like, luminal A, luminal B, Her2, normal-like, and claudin-low.

Basal-like breast cancer (BLBC) is an especially aggressive form of the disease, and BLBC patients generally have a poor prognosis. Following [Wu and Smyth \(2012\)](#), we define a binary response vector to indicate whether or not samples are BLBC. Gene sets were downloaded from the curated C2 collection of the MSigDB and tested for their association with this dichotomous outcome.

We trained a series of RF classifiers to predict BLBC based on microarray data. Null models were built for each of the 2,609 gene sets in the C2 collection for which at least 25 genes were present in the expression matrix. Each forest contains 10,000 trees. Models were evaluated using the CE loss function on out-of-bag samples.

We calculate  $p$ -values for each  $\text{CPI}_\lambda$  via the  $t$ -test and corresponding  $q$ -values using the Benjamini-Hochberg algorithm (Benjamini and Hochberg, 1995). We identify 75 significantly enriched gene sets at  $q \leq 0.05$ , including 13 of 73 explicitly breast cancer derived gene sets and 6 of 13 gene sets indicative of basal signatures. Almost all top results are from cancer studies or other biologically relevant research (see Fig. 4). These include 2 sets of BRCA1 targets, genetic mutations known to be associated with BLBC (Turner and Reis-Filho, 2006), and 5 sets of ESR1 targets, which are known markers for the luminal A subtype (Sørlie et al., 2003).

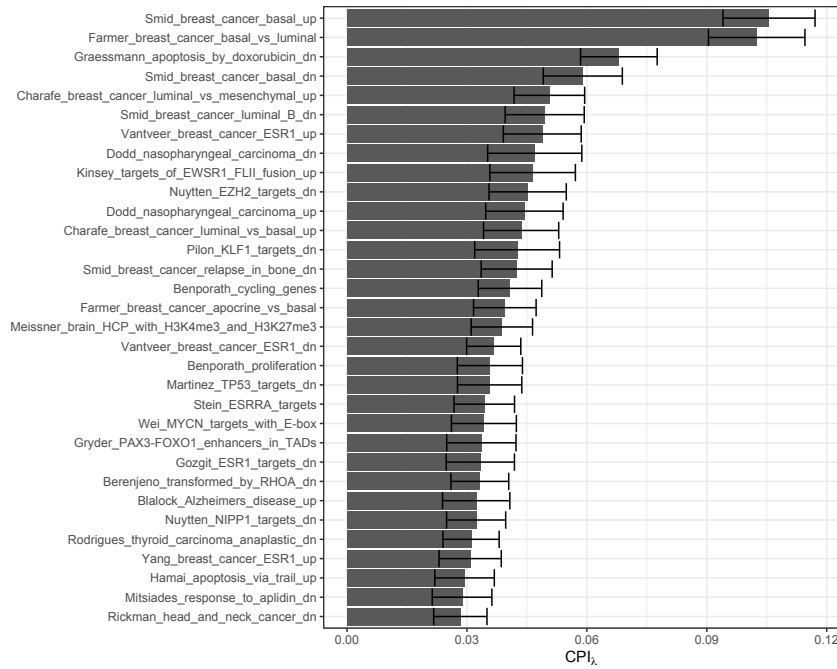


FIG 4. Results for all 32 gene sets in the MSigDB's C2 collection that passed a 1% FDR threshold. Whiskers represent standard errors.

These results are similar to those from popular pathway enrichment tests like GSEA (Subramanian et al., 2005) and CAMERA (Wu and Smyth, 2012), which respectively identify 137 and 74 differentially enriched pathways in this dataset at 5% FDR. The overlap is notable given that those methods rely on marginal associations between gene expression and clinical outcomes, whereas the CPI is a conditional test with a more restrictive null hypothesis, and should theoretically have less power to detect enrichment when features within a gene set are correlated with others outside it. De-

spite collinearity between genes, the CPI still identifies a large number of biologically meaningful gene sets differentiating BLBC tumors from other breast cancer subtypes.

**5. Discussion.** The two measures introduced in this paper have commonsense interpretations.  $\text{CPI}_\Delta$  quantifies the improvement in model performance when incorporating the information in  $\mathbf{X}^S$ , as measured in units of loss. This measure is appropriate when we expect our submatrix of interest to have an additive effect on predictive performance.

The interpretation of  $\text{CPI}_\lambda$  is somewhat less straightforward. Log-ratios are not as easily graspable as differences, but with a simple transformation we may convert  $\text{CPI}_\lambda$  into a proportional reduction in error (PRE) statistic:  $\text{PRE} = 1 - e^{-\text{CPI}_\lambda}$ . Under this transformation,  $\text{CPI}_\lambda$  can be used to quantify the percent of the null model’s loss that is eliminated by incorporating the information in  $\mathbf{X}^S$ . This measure is appropriate when we expect our submatrix of interest to have a multiplicative effect on predictive performance.

Note that the two measures are not rank-equivalent. This is because  $R_{\text{emp}}(f_0, \tilde{\mathbf{Z}})$  puts an upper bound on  $\text{CPI}_\Delta$ , whereas  $\text{CPI}_\lambda$  can be arbitrarily high for any  $R_{\text{emp}}(f_0, \tilde{\mathbf{Z}})$ , provided  $R_{\text{emp}}(f, \mathbf{Z})$  is sufficiently small. A scatter plot of the two variables on a simulated dataset demonstrates the bow-like relationship between them, as the values cluster together near the origin but fan out across quadrants I and III of the Cartesian plane (see Fig. 5).

**6. Conclusion.** We propose the conditional predictive impact (CPI), a maximally general test of conditional independence. It works with continuous and categorical predictors in regression and classification settings using any supervised learning algorithm and loss function. It imposes no parametric or sparsity constraints, and can be efficiently computed on data with many observations and features.

The cost for this generality is either imperfect error control (as with  $\text{CPI}_\Delta$ ) or suboptimal statistical power (as with  $\text{CPI}_\lambda$ ). This kind of sensitivity/specificity trade-off is common in machine learning. [Shah and Peters \(2018\)](#) have demonstrated that no CI test can be uniformly valid against arbitrary alternatives, a sort of no-free-lunch theorem for CI. However, we have shown that our approach is consistent and unbiased under minimal assumptions. Empirical results demonstrate that our method performs favorably against a number of alternatives for a range of supervised learners and data generating processes.

We envision several avenues for future research in this area. Localized versions of the CPI algorithm could be used to detect the conditional importance of features on particular predictions. Model-specific methods could be

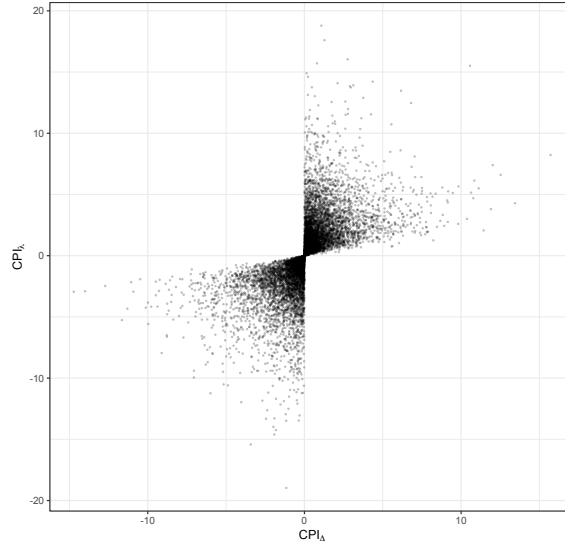


FIG 5. Scatter plot of 10,000 simulated values of  $CPI_{\Delta}$  vs.  $CPI_{\lambda}$ . There is a clear positive association between the two measures (Pearson  $\rho = 0.628$ ; Spearman  $\rho = 0.870$ ), though the relationship is not perfectly monotonic.

implemented to speed up the procedure. We are currently working on applications for causal inference and estimation, an especially promising direction for this approach.

## References.

- BACH, S., BINDER, A., MONTAVON, G., KLAUSCHEN, F., MÜLLER, K. R. and SAMEK, W. (2015). On pixel-wise explanations for non-linear classifier decisions by layer-wise relevance propagation. *PLoS ONE* **10** 1–46.
- BARBER, R. F. and CANDÈS, E. J. (2015). Controlling the false discovery rate via knockoffs. *Ann. Statist.* **43** 2055–2085.
- BENJAMINI, Y. and HOCHBERG, Y. (1995). Controlling the false discovery rate: a practical and powerful approach to multiple testing. *J. Royal Stat. Soc. Ser. B. Methodol.* **57** 289–300.
- BISCHL, B., LANG, M., KOTTHOFF, L., SCHIFFNER, J., RICHTER, J., STUDERUS, E., CASALICCHIO, G. and JONES, Z. M. (2016). mlr: Machine learning in R. *J. Mach. Learn. Res.* **17** 1–5.
- BREIMAN, L. (2001). Random forests. *Mach. Learn.* **45** 1–33.
- CANDÈS, E., FAN, Y., JANSON, L. and LV, J. (2018). Panning for gold: ‘model-X’ knockoffs for high dimensional controlled variable selection. *J. Royal Stat. Soc. Ser. B. Methodol.* **80** 551–577.
- CHALUPKA, K., PERONA, P. and EBERHARDT, F. (2018). Fast conditional independence test for vector variables with large sample sizes. Preprint. Available at [arXiv:1804.02747](https://arxiv.org/abs/1804.02747).

- DATTA, A., SEN, S. and ZICK, Y. (2016). Algorithmic transparency via quantitative input influence: Theory and experiments with learning systems. *2016 IEEE Symposium on Security and Privacy* 598–617.
- DORAN, G., MUANDET, K., ZHANG, K. and SCHÖLKOPF, B. (2014). A permutation-based kernel conditional independence test. In *Proceedings of the Thirtieth Conference on Uncertainty in Artificial Intelligence. UAI'14* 132–141. AUAI Press, Arlington, Virginia, United States.
- DUA, D. and TANISKIDOU, K. (2017). *UCI Machine Learning Repository*. University of California, School of Information and Computer Science, Irvine, CA.
- FENG, J., WILLIAMSON, B., SIMON, N. and CARONE, M. (2018). Nonparametric variable importance using an augmented neural network with multi-task learning. In *Proceedings of the 35th International Conference on Machine Learning* (J. DY and A. KRAUSE, eds.). *Proceedings of Machine Learning Research* **80** 1496–1505. PMLR, Stockholmsmässan, Stockholm Sweden.
- FISHER, R. A. (1935). *The Design of Experiments*. Oliver & Boyd, London.
- FISHER, A., RUDIN, C. and DOMINICI, F. (2018). All Models are Wrong but Many are Useful: Variable Importance for Black-Box, Proprietary, or Misspecified Prediction Models, using Model Class Reliance. Preprint. Available at [arXiv:1801.01489v3](https://arxiv.org/abs/1801.01489v3).
- FRIEDMAN, J. H. and POPESCU, B. E. (2008). Predictive learning via rule ensembles. *Ann. Appl. Stat.* **2** 916–954.
- FUKUMIZU, K., GRETTON, A., SUN, X. and SCHÖLKOPF, B. (2008). Kernel measures of conditional dependence. In *Advances in Neural Information Processing Systems 20* (J. C. Platt, D. Koller, Y. Singer and S. T. Roweis, eds.) 489–496. Curran Associates, Inc.
- GERMAIN, P., BACH, F., LACOSTE, A. and LACOSTE-JULIEN, S. (2016). PAC-Bayesian Theory Meets Bayesian Inference. In *Advances in Neural Information Processing Systems 29* (D. D. Lee, M. Sugiyama, U. V. Luxburg, I. Guyon and R. Garnett, eds.) 1884–1892. Curran Associates, Inc.
- GEVREY, M., DIMOPOULOS, I. and LEK, S. (2003). Review and comparison of methods to study the contribution of variables in artificial neural network models. *Ecol. Model.* **160** 249–264.
- GREGORUTTI, B., MICHEL, B. and SAINT-PIERRE, P. (2015). Grouped variable importance with random forests and application to multiple functional data analysis. *Comput. Stat. Data Anal.* **90** 15–35.
- GRÖMPING, U. (2007). Estimators of relative importance in linear regression based on variance decomposition. *Am. Stat.* **61** 139–147.
- GUO, C., PLEISS, G., SUN, Y. and WEINBERGER, K. (2017). On calibration of modern neural networks. Preprint. Available at [arXiv:1706.04599v2](https://arxiv.org/abs/1706.04599v2).
- HARRISON, D. and RUBINFELD, D. L. (1978). Hedonic housing prices and the demand for clean air. *J. Environ. Econ. Manag.* **5** 81–102.
- HERSCHKOWITZ, J. I., SIMIN, K., WEIGMAN, V. J., MIKAELIAN, I., USARY, J., HU, Z., RASMUSSEN, K. E., JONES, L. P., ASSEFNIA, S., CHANDRASEKHARAN, S., BACKLUND, M. G., YIN, Y., KHRAMTSOV, A. I., BASTEIN, R., QUACKENBUSH, J., GLAZER, R. I., BROWN, P. H., GREEN, J. E., KOPELOVICH, L., FURTH, P. A., PALAZZO, J. P., OLOPADE, O. I., BERNARD, P. S., CHURCHILL, G. A., VAN DYKE, T. and PEROU, C. M. (2007). Identification of conserved gene expression features between murine mammary carcinoma models and human breast tumors. *Genome Biol.* **8** R76.
- HOLM, S. (1979). A simple sequentially rejective multiple test procedure. *Scand. J. Stat.* **6** 65–70.
- HUBBARD, A. E., KENNEDY, C. J. and VAN DER LAAN, M. J. (2018). Data-adaptive target

- parameters. In *Targeted Learning in Data Science* (M. J. van der Laan and S. Rose, eds.) 9, 125–142. Springer, New York.
- KALISCH, M., MÄCHLER, M., COLOMBO, D., MAATHUIS, M. H. and BÜHLMANN, P. (2012). Causal inference using graphical models with the R package pcalg. *J. Stat. Softw.* **47** 1–26.
- KOLLER, D. and FRIEDMAN, N. (2009). *Probabilistic Graphical Models: Principles and Techniques*. MIT Press, Cambridge, MA.
- KORB, K. B. and NICHOLSON, A. E. (2009). *Bayesian Artificial Intelligence*, 2nd ed. Chapman and Hall/CRC, Boca Raton, FL.
- KRUSCHKE, J. K. (2013). Bayesian estimation supersedes the t test. *J. Exp. Psychol. Gen.* **142** 573.
- KURSA, M. B. and RUDNICKI, W. R. (2010). Feature selection with the boruta package. *J. Stat. Softw.* **36**.
- LIM, E., VAILLANT, F., WU, D., FORREST, N. C., PAL, B., HART, A. H., ASSELIN-LABAT, M.-L., GYORKI, D. E., WARD, T., PARTANEN, A., FELEPPA, F., HUSCHTSCHA, L. I., THORNE, H. J., KCONFAB, FOX, S. B., YAN, M., FRENCH, J. D., BROWN, M. A., SMYTH, G. K., VISVADER, J. E. and LINDEMAN, G. J. (2009). Aberrant luminal progenitors as the candidate target population for basal tumor development in BRCA1 mutation carriers. *Nat. Med.* **15** 907.
- LINDEMAN, R. H., MERENDA, P. F. and GOLD, R. Z. (1980). *Introduction to Bivariate and Multivariate Analysis*. Longman, Glenview, IL.
- LUNDBERG, S. and LEE, S.-I. (2017). A unified approach to interpreting model predictions. Preprint. Available at [arXiv:1705.07874](https://arxiv.org/abs/1705.07874).
- MAATHUIS, M. H., KALISCH, M. and BÜHLMANN, P. (2009). Estimating high-dimensional intervention effects from observational data. *Ann. Statist.* **37** 3133–3164.
- MENTCH, L. and HOOKER, G. (2016). Quantifying uncertainty in random forests via confidence intervals and hypothesis tests. *J. Mach. Learn. Res.* **17** 841–881.
- MEYER, D., DIMITRIADOU, E., HORNIK, K., WEINGESSEL, A. and LEISCH, F. (2018). e1071: Misc Functions of the Department of Statistics, Probability Theory Group (Formerly: E1071), TU Wien. R package version 1.7-0.
- NICODEMUS, K. K., MALLEY, J. D., STROBL, C. and ZIEGLER, A. (2010). The behaviour of random forest permutation-based variable importance measures under predictor correlation. *BMC Bioinform.* **11** 110.
- NICULESCU-MIZIL, A. and CARUANA, R. (2005). Predicting Good Probabilities with Supervised Learning. In *Proceedings of the 22Nd International Conference on Machine Learning. ICML '05* 625–632. ACM, New York, NY, USA.
- PHIPSON, B. and SMYTH, G. (2010). Permutation P-values should never be zero: calculating exact P-values when permutations are randomly drawn. *Stat. Appl. Genet. Mol. Biol.* **9**.
- RAMSEY, J. D. (2014). A scalable conditional independence test for nonlinear, non-gaussian data. Preprint. Available at [arXiv:1401.5031v2](https://arxiv.org/abs/1401.5031v2).
- RIBEIRO, M. T., SINGH, S. and GUESTRIN, C. (2016). "Why Should I Trust You?": Explaining the predictions of any classifier. Preprint. Available at [arXiv:1602.04938](https://arxiv.org/abs/1602.04938).
- ROUDER, J. N., SPECKMAN, P. L., SUN, D., MOREY, R. D. and IVERSON, G. (2009). Bayesian t tests for accepting and rejecting the null hypothesis. *Psychon. Bull. Rev.* **16** 225–237.
- SAUER, N. (1972). On the density of families of sets. *J. Comb. Theory Ser. A* **13** 145–147.
- SCUTARI, M. (2010). Learning Bayesian networks with the bnlearn R package. *J. Stat. Softw.* **35** 1–22.
- SCUTARI, M. and DENIS, J.-B. (2014). *Bayesian Networks: With Examples in R*. Chapman

- and Hall/CRC, Boca Raton, FL.
- SHAH, R. and PETERS, J. (2018). The hardness of conditional independence testing and the generalised covariance measure. Preprint. Available at [arXiv:1804.07203v2](https://arxiv.org/abs/1804.07203v2).
- SHELAK, S. (1972). A combinatorial problem: stability and orders for models and theories in infinitary languages. *Pac. J. Math.* **41** 247–261.
- SHRIKUMAR, A., GREENSIDE, P. and KUNDAJE, A. (2017). Learning important features through propagating activation differences. Preprint. Available at [arXiv:1704.02685](https://arxiv.org/abs/1704.02685).
- SØRLIE, T., TIBSHIRANI, R., PARKER, J., HASTIE, T., MARRON, J. S., NOBEL, A., DENG, S., JOHNSEN, H., PESICH, R., GEISLER, S., DEMETER, J., PEROU, C. M., LØNNING, P. E., BROWN, P. O., BØRRESEN-DALE, A.-L. and BOTSTEIN, D. (2003). Repeated observation of breast tumor subtypes in independent gene expression data sets. *Proc. Natl. Acad. Sci.* **100** 8418 LP – 8423.
- SPIRITES, P., GLYMOUR, C. N. and SCHEINES, R. (2000). *Causation, Prediction, and Search*, 2nd ed. MIT Press, Cambridge, MA.
- STROBL, E. V., ZHANG, K. and VISWESWARAN, S. (2017). Approximate kernel-based conditional independence tests for fast non-parametric causal discovery. Preprint. Available at [arXiv:1702.03877v2](https://arxiv.org/abs/1702.03877v2).
- STROBL, C., BOULESTEIX, A.-L., KNEIB, T., AUGUSTIN, T. and ZEILEIS, A. (2008). Conditional variable importance for random forests. *BMC Bioinform.* **9** 307.
- SUBRAMANIAN, A., TAMAYO, P., MOOTHA, V. K., MUKHERJEE, S., EBERT, B. L. and GILLETTE, M. A. (2005). Gene set enrichment analysis: A knowledge-based approach for interpreting genome-wide expression profiles. *Proc. Natl. Acad. Sci.* **102** 15545–15550.
- R CORE TEAM (2018). R: A Language and Environment for Statistical Computing. Vienna, Austria.
- TURNER, N. C. and REIS-FILHO, J. S. (2006). Basal-like breast cancer and the BRCA1 phenotype. *Oncogene* **25** 5846.
- VALIANT, L. G. (1984). A theory of the learnable. *Commun. ACM* **27** 1134–1142.
- VAN DER LAAN, M. J. (2006). Statistical inference for variable importance. *Int. J. Biostat.* **2**.
- VAN DER LAAN, M. J. and ROSE, S., eds. (2018). *Targeted Learning in Data Science*. Springer, New York.
- VAPNIK, V. (1998). *Statistical Learning Theory*. John Wiley & Sons, New York.
- VAPNIK, V. and CHERVONENKIS, A. (1971). On the uniform convergence of relative frequencies to their probabilities. *Theory Probab. Appl.* **16** 264–280.
- VENABLES, W. N. and RIPLEY, B. D. (2002). *Modern Applied Statistics with S*, 4th ed. Springer, New York.
- VERMA, T. and PEARL, J. (1991). Equivalence and Synthesis of Causal Models. In *Proceedings of the Sixth Annual Conference on Uncertainty in Artificial Intelligence. UAI '90* 255–270. Elsevier Science Inc., New York, NY, USA.
- WACHTER, S., MITTELSTADT, B. and RUSSELL, C. (2017). Counterfactual explanations without opening the black box: Automated decisions and the GDPR. Preprint. Available at [arXiv:1711.00399](https://arxiv.org/abs/1711.00399).
- WETZELS, R., RAAIJMAKERS, J. G. W., JAKAB, E. and WAGENMAKERS, E.-J. (2009). How to quantify support for and against the null hypothesis: A flexible WinBUGS implementation of a default Bayesian t test. *Psychon. Bull. Rev.* **16** 752–760.
- WILKS, S. S. (1938). The large-sample distribution of the likelihood ratio for testing composite hypotheses. *Ann. Math. Stat.* **9** 60–62.
- WILLIAMSON, B., GILBERT, P., SIMON, N. and CARONE, M. (2017). Nonparametric variable importance assessment using machine learning techniques. Preprint. Available at

[UW Biostatistics Working Paper 422.](#)

WRIGHT, M. N. and ZIEGLER, A. (2017). ranger: A fast implementation of random forests for high dimensional data in C++ and R. *J. Stat. Softw.* **77**.

WU, D. and SMYTH, G. K. (2012). Camera: a competitive gene set test accounting for inter-gene correlation. *Nucleic Acids Res.* **40** e133.

ZHANG, K., PETERS, J., JANZING, D. and SCHOELKOPF, B. (2012). Kernel-based conditional independence test and application in causal discovery. Preprint. Available at [arXiv:1202.3775](#).

DAVID S. WATSON  
OXFORD INTERNET INSTITUTE  
UNIVERSITY OF OXFORD  
1 SAINT GILES'  
OXFORD OX1 3JS  
AND  
THE ALAN TURING INSTITUTE  
96 EUSTON ROAD  
LONDON NW1 2DB  
E-MAIL: [david.watson@oii.ox.ac.uk](mailto:david.watson@oii.ox.ac.uk)

MARVIN N. WRIGHT  
LEIBNIZ INSTITUTE FOR PREVENTION  
RESEARCH AND EPIDEMIOLOGY – BIPS  
BREMEN, GERMANY  
AND  
SECTION OF BIOSTATISTICS  
DEPARTMENT OF PUBLIC HEALTH  
UNIVERSITY OF COPENHAGEN  
COPENHAGEN, DENMARK  
E-MAIL: [wright@leibniz-bips.de](mailto:wright@leibniz-bips.de)



# Supplementary material for “Testing Conditional Independence in Supervised Learning Algorithms”

David S. Watson and Marvin N. Wright

December 15, 2024

Learner	Linear data		Non-linear data	
	<i>t</i> -Test	Fisher	<i>t</i> -Test	Fisher
Linear model	0.9488	0.9493	0.9522	0.9494
Support vector machine	0.9325	0.9362	0.9387	0.9335
Random forest	0.9497	0.9464	0.9500	0.9466
Neural network	0.9451	0.9456	0.9441	0.9404

Table S1: Empirical coverage probabilities of 95% confidence intervals in the simulation study, calculated from 10,000 simulation replicates; continuous outcome with MSE loss function; multiplicative CPI.

Learner	Linear data		Non-linear data	
	<i>t</i> -Test	Fisher	<i>t</i> -Test	Fisher
Linear model	0.9493	0.9469	0.9496	0.9483
Support vector machine	0.9347	0.9337	0.9314	0.9340
Random forest	0.9489	0.9523	0.9466	0.9488
Neural network	0.9435	0.9402	0.9429	0.9432

Table S2: Empirical coverage probabilities of 95% confidence intervals in the simulation study, calculated from 10,000 simulation replicates; continuous outcome with MAE loss function; multiplicative CPI.

Learner	Linear data		Non-linear data	
	<i>t</i> -Test	Fisher	<i>t</i> -Test	Fisher
Linear model	0.9573	0.9578	0.9546	0.9551
Support vector machine	0.9219	0.9200	0.9111	0.9098
Random forest	0.9407	0.9431	0.9312	0.9345
Neural network	0.9223	0.9204	0.9100	0.9127

Table S3: Empirical coverage probabilities of 95% confidence intervals in the simulation study, calculated from 10,000 simulation replicates; continuous outcome with MSE loss function; additive CPI.

Learner	Linear data		Non-linear data	
	<i>t</i> -Test	Fisher	<i>t</i> -Test	Fisher
Linear model	0.9537	0.9516	0.9536	0.9544
Support vector machine	0.9037	0.9050	0.8995	0.8989
Random forest	0.9415	0.9377	0.9385	0.9366
Neural network	0.9222	0.9267	0.9211	0.9170

Table S4: Empirical coverage probabilities of 95% confidence intervals in the simulation study, calculated from 10,000 simulation replicates; continuous outcome with MAE loss function; additive CPI.

Learner	Linear data		Non-linear data	
	<i>t</i> -Test	Fisher	<i>t</i> -Test	Fisher
Logistic regression	0.9243	0.9516	0.9269	0.9353
Support vector machine	0.9216	0.9351	0.9220	0.9362
Random forest	0.9403	0.9480	0.9356	0.9503
Neural network	0.9358	0.9415	0.9353	0.9453

Table S5: Empirical coverage probabilities of 95% confidence intervals in the simulation study, calculated from 10,000 simulation replicates; classification outcome with MMCE loss function; multiplicative CPI.

Learner	Linear data		Non-linear data	
	<i>t</i> -Test	Fisher	<i>t</i> -Test	Fisher
Logistic regression	0.8807	0.8806	0.8910	0.8867
Support vector machine	0.7653	0.7702	0.7642	0.7634
Random forest	0.9285	0.9293	0.9185	0.9190
Neural network	0.8547	0.8550	0.8767	0.8788

Table S6: Empirical coverage probabilities of 95% confidence intervals in the simulation study, calculated from 10,000 simulation replicates; classification outcome with CE loss function; multiplicative CPI.

Learner	Linear data		Non-linear data	
	<i>t</i> -Test	Fisher	<i>t</i> -Test	Fisher
Logistic regression	0.9258	0.9518	0.9274	0.9387
Support vector machine	0.9219	0.9345	0.9217	0.9351
Random forest	0.9398	0.9448	0.9362	0.9500
Neural network	0.9325	0.9392	0.9343	0.9454

Table S7: Empirical coverage probabilities of 95% confidence intervals in the simulation study, calculated from 10,000 simulation replicates; classification outcome with MMCE loss function; additive CPI.

Learner	Linear data		Non-linear data	
	<i>t</i> -Test	Fisher	<i>t</i> -Test	Fisher
Logistic regression	0.9567	0.9596	0.9535	0.9591
Support vector machine	0.8979	0.8931	0.8878	0.8941
Random forest	0.9435	0.9404	0.9412	0.9402
Neural network	0.9147	0.9171	0.9276	0.9233

Table S8: Empirical coverage probabilities of 95% confidence intervals in the simulation study, calculated from 10,000 simulation replicates; classification outcome with CE loss function; additive CPI.

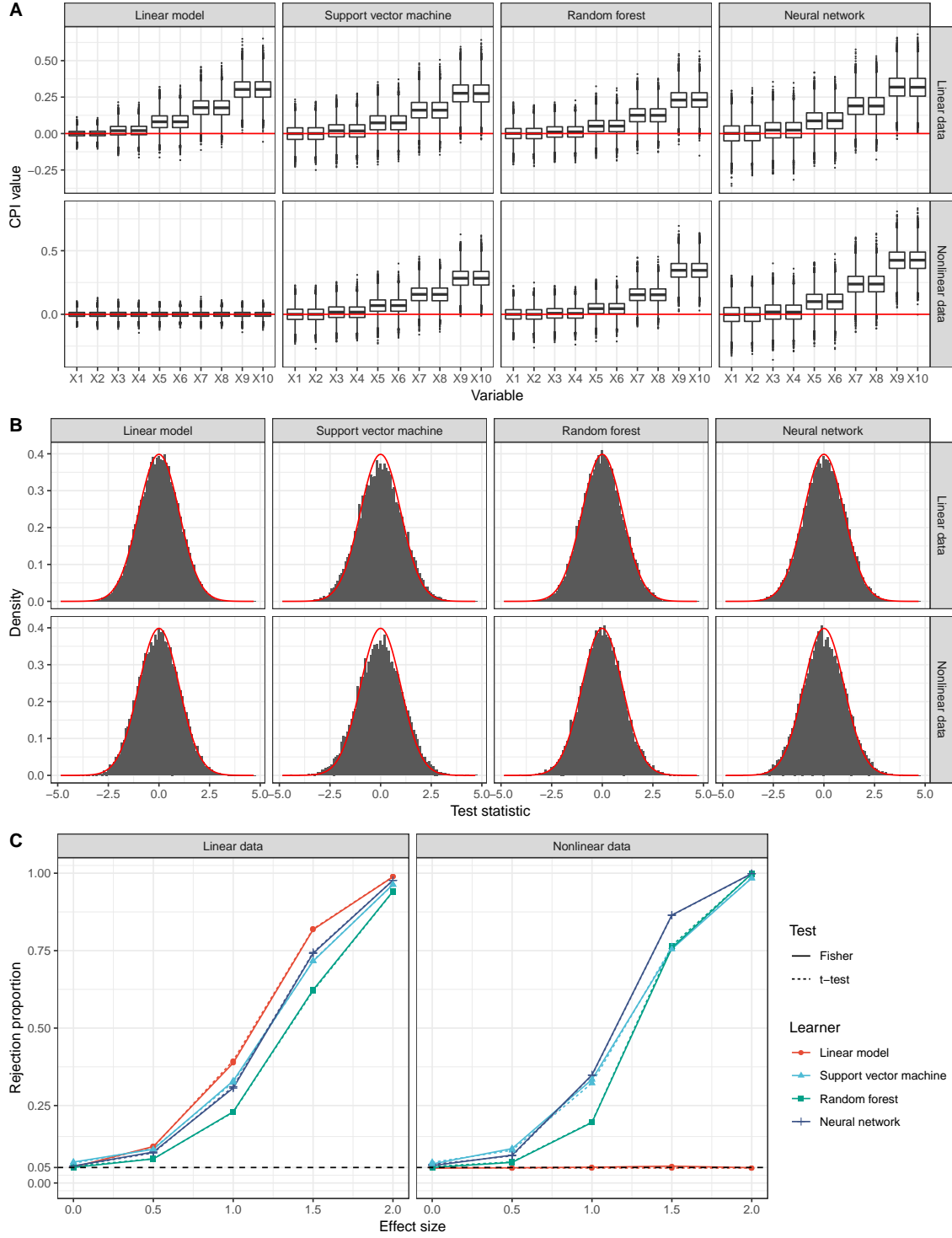


Figure S1: Simulation results for continuous outcome with MSE loss function and multiplicative version of CPI. **A**: Boxplots of simulation replications of CPI values of variables  $X_1, \dots, X_{10}$  with increasing effect size. The red line indicates a CPI value of 0, corresponding to no estimated association between the variable  $X_j$  and the outcome  $Y$ . **B**: Histograms of simulation replications of  $t$ -statistics of variables with effect size 0. The distribution of the expected  $t$ -statistic under the null hypothesis is shown in red. **C**: Average proportion of rejected hypotheses at  $\alpha = 0.05$ . Results at effect size 0 correspond to the type I error, at effect sizes  $> 0$  to statistical power. The dashed line indicates the nominal level of  $\alpha = 0.05$ . The panels correspond to the simulation scenario, the colors and symbols to the learning algorithms and the line types to the inference procedure.

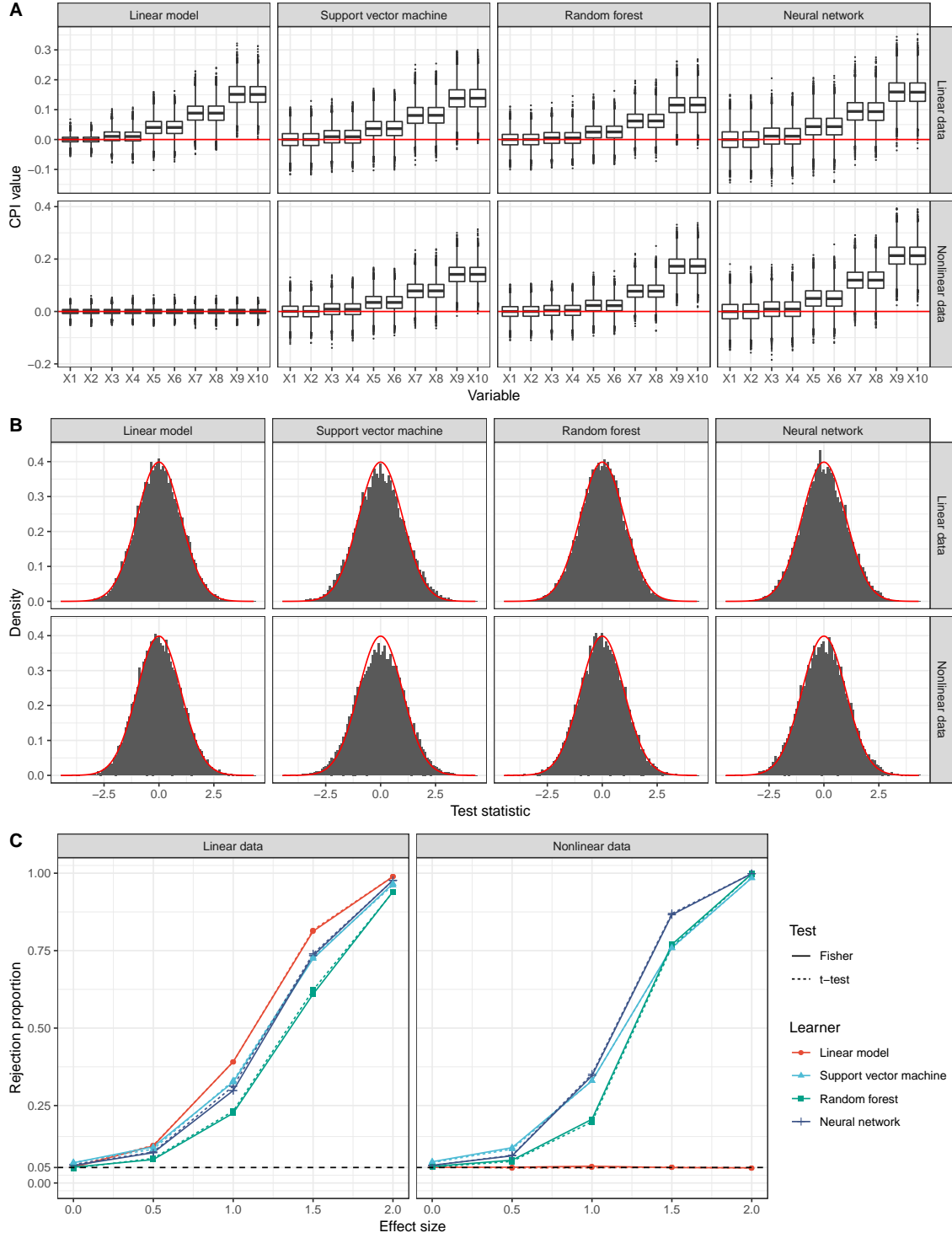


Figure S2: Simulation results for continuous outcome with MAE loss function and multiplicative version of CPI. **A**: Boxplots of simulation replications of CPI values of variables  $X_1, \dots, X_{10}$  with increasing effect size. The red line indicates a CPI value of 0, corresponding to no estimated association between the variable  $X_j$  and the outcome  $Y$ . **B**: Histograms of simulation replications of  $t$ -statistics of variables with effect size 0. The distribution of the expected  $t$ -statistic under the null hypothesis is shown in red. **C**: Average proportion of rejected hypotheses at  $\alpha = 0.05$ . Results at effect size 0 correspond to the type I error, at effect sizes  $> 0$  to statistical power. The dashed line indicates the nominal level of  $\alpha = 0.05$ . The panels correspond to the simulation scenario, the colors and symbols to the learning algorithms and the line types to the inference procedure.

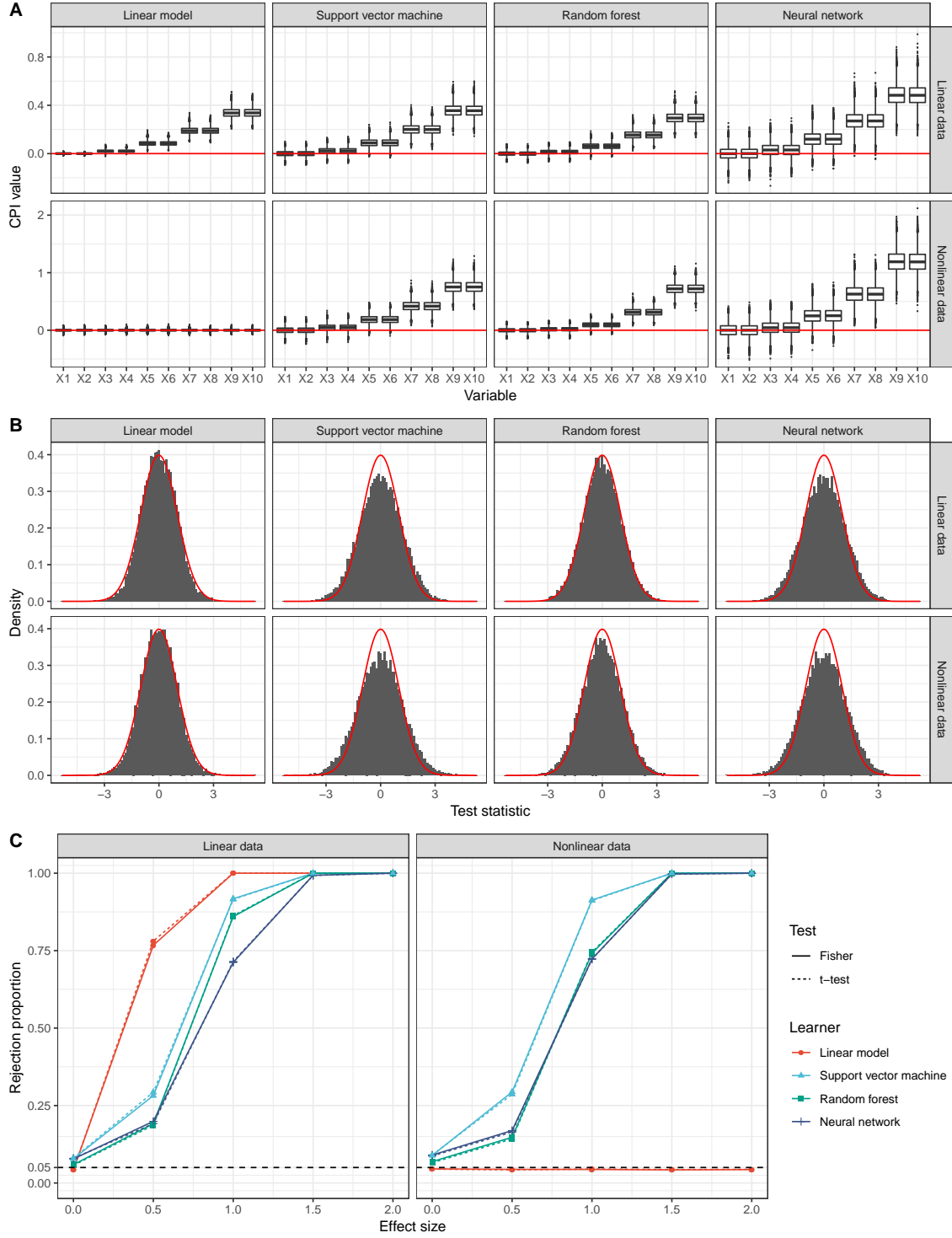


Figure S3: Simulation results for continuous outcome with MSE loss function and additive version of CPI. **A**: Boxplots of simulation replications of CPI values of variables  $X_1, \dots, X_{10}$  with increasing effect size. The red line indicates a CPI value of 0, corresponding to no estimated association between the variable  $X_j$  and the outcome  $Y$ . **B**: Histograms of simulation replications of  $t$ -statistics of variables with effect size 0. The distribution of the expected  $t$ -statistic under the null hypothesis is shown in red. **C**: Average proportion of rejected hypotheses at  $\alpha = 0.05$ . Results at effect size 0 correspond to the type I error, at effect sizes  $> 0$  to statistical power. The dashed line indicates the nominal level of  $\alpha = 0.05$ . The panels correspond to the simulation scenario, the colors and symbols to the learning algorithms and the line types to the inference procedure.

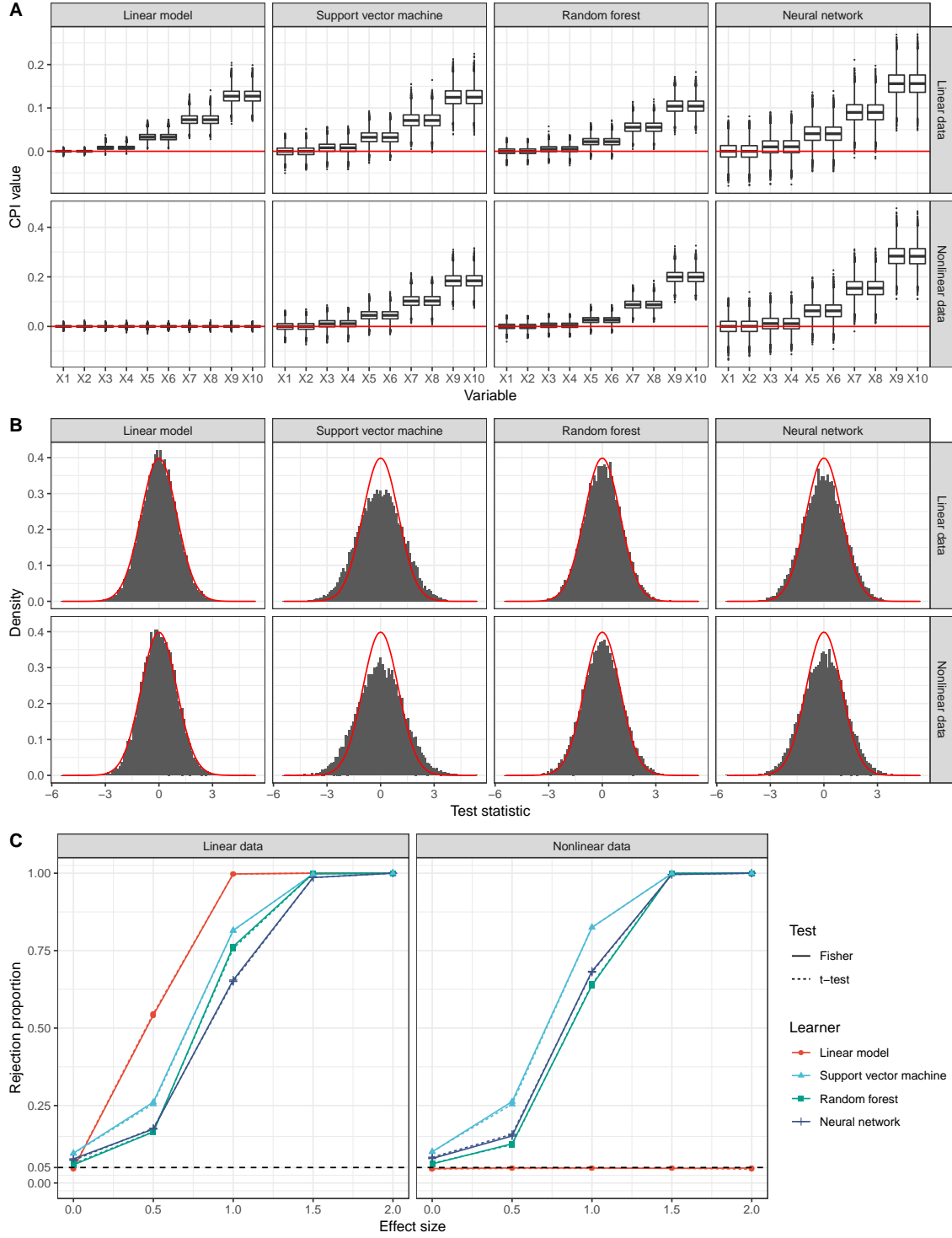


Figure S4: Simulation results for continuous outcome with MAE loss function and additive version of CPI. **A**: Boxplots of simulation replications of CPI values of variables  $X_1, \dots, X_{10}$  with increasing effect size. The red line indicates a CPI value of 0, corresponding to no estimated association between the variable  $X_j$  and the outcome  $Y$ . **B**: Histograms of simulation replications of  $t$ -statistics of variables with effect size 0. The distribution of the expected  $t$ -statistic under the null hypothesis is shown in red. **C**: Average proportion of rejected hypotheses at  $\alpha = 0.05$ . Results at effect size 0 correspond to the type I error, at effect sizes  $> 0$  to statistical power. The dashed line indicates the nominal level of  $\alpha = 0.05$ . The panels correspond to the simulation scenario, the colors and symbols to the learning algorithms and the line types to the inference procedure.

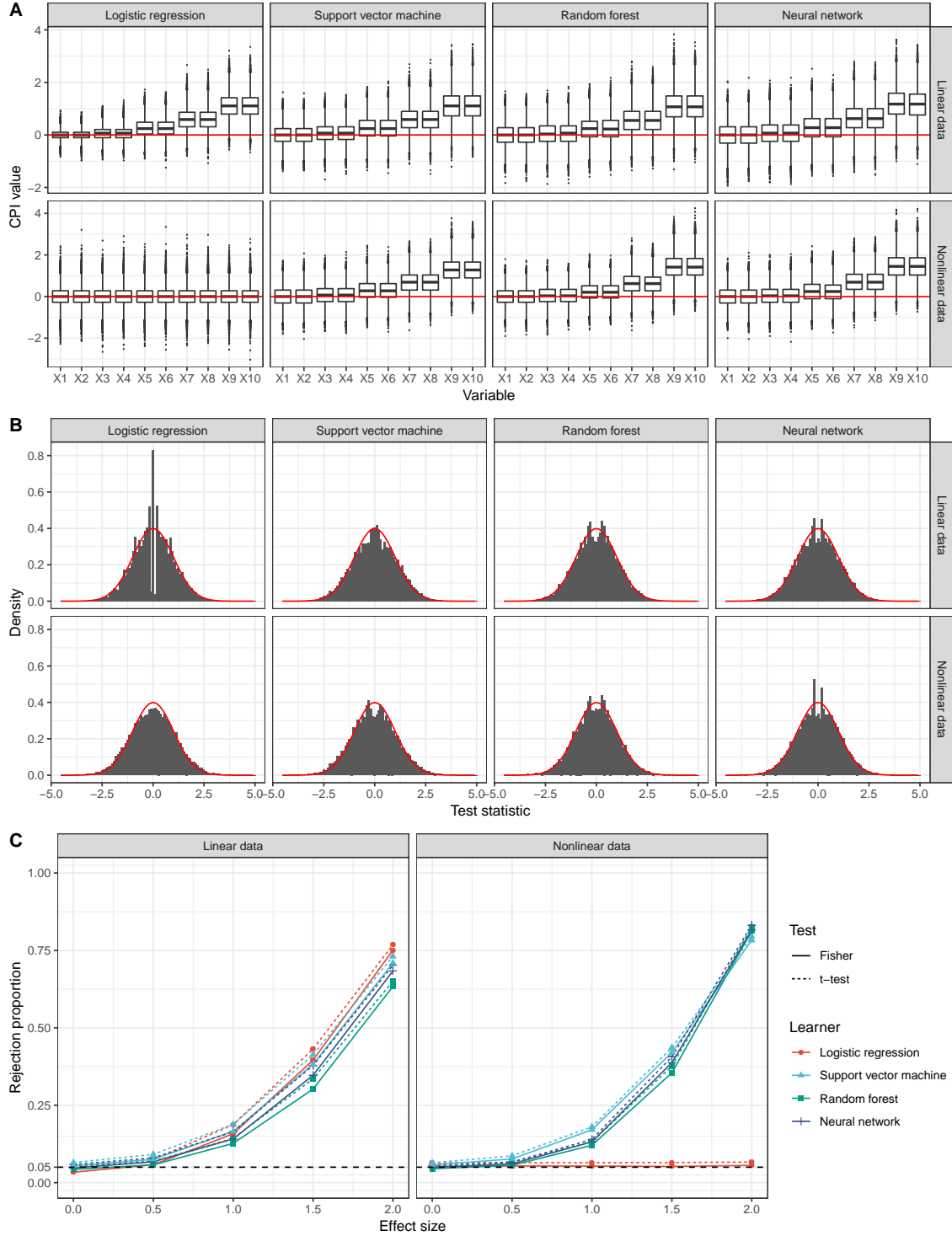


Figure S5: Simulation results for classification outcome with MMCE loss function and multiplicative version of CPI. **A:** Boxplots of simulation replications of CPI values of variables  $X_1, \dots, X_{10}$  with increasing effect size. The red line indicates a CPI value of 0, corresponding to no estimated association between the variable  $X_j$  and the outcome  $Y$ . **B:** Histograms of simulation replications of  $t$ -statistics of variables with effect size 0. The distribution of the expected  $t$ -statistic under the null hypothesis is shown in red. **C:** Average proportion of rejected hypotheses at  $\alpha = 0.05$ . Results at effect size 0 correspond to the type I error, at effect sizes  $> 0$  to statistical power. The dashed line indicates the nominal level of  $\alpha = 0.05$ . The panels correspond to the simulation scenario, the colors and symbols to the learning algorithms and the line types to the inference procedure.

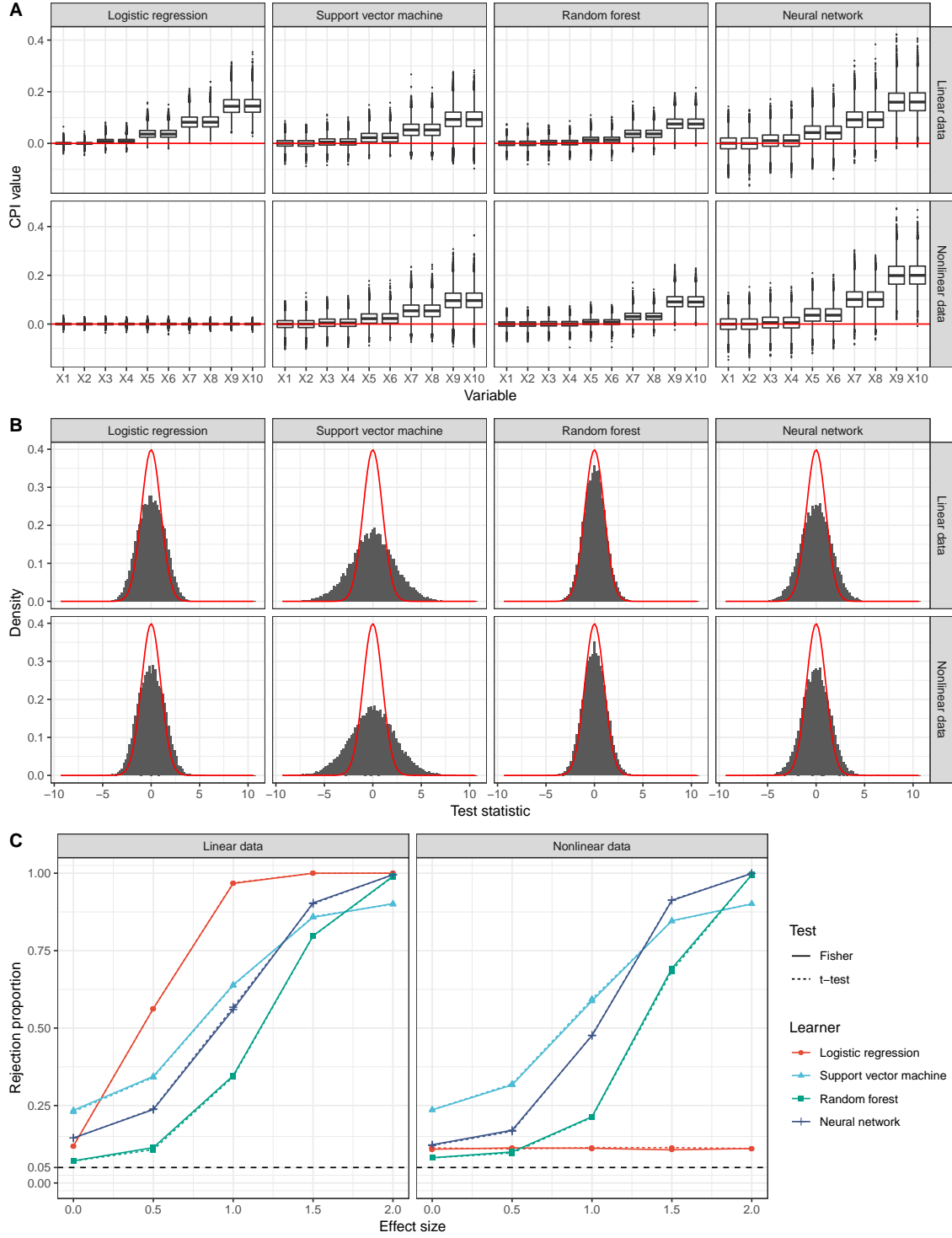


Figure S6: Simulation results for classification outcome with CE loss function and multiplicative version of CPI. **A**: Boxplots of simulation replications of CPI values of variables  $X_1, \dots, X_{10}$  with increasing effect size. The red line indicates a CPI value of 0, corresponding to no estimated association between the variable  $X_j$  and the outcome  $Y$ . **B**: Histograms of simulation replications of  $t$ -statistics of variables with effect size 0. The distribution of the expected  $t$ -statistic under the null hypothesis is shown in red. **C**: Average proportion of rejected hypotheses at  $\alpha = 0.05$ . Results at effect size 0 correspond to the type I error, at effect sizes  $> 0$  to statistical power. The dashed line indicates the nominal level of  $\alpha = 0.05$ . The panels correspond to the simulation scenario, the colors and symbols to the learning algorithms and the line types to the inference procedure.



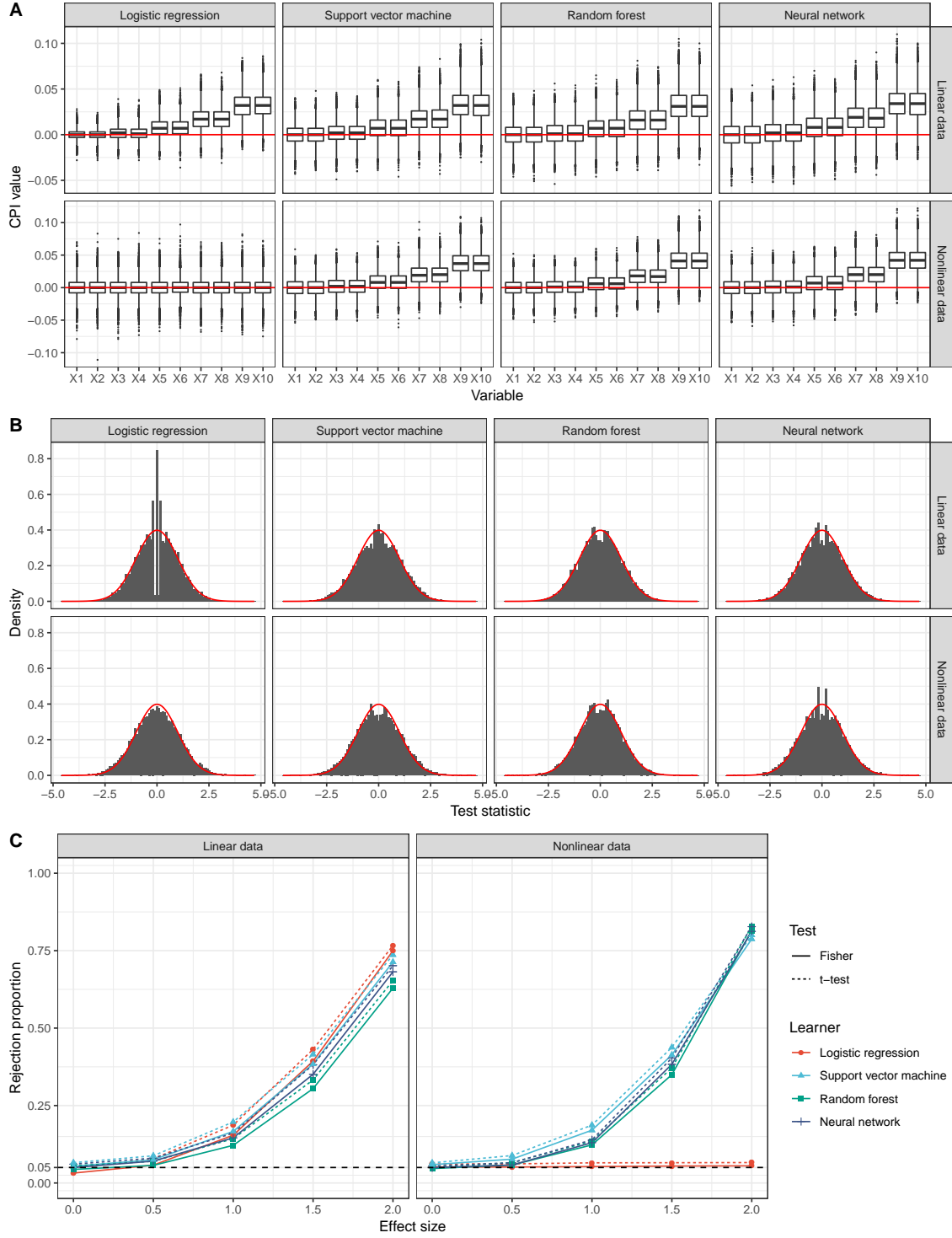


Figure S7: Simulation results for classification outcome with MMCE loss function and additive version of CPI. **A**: Boxplots of simulation replications of CPI values of variables  $X_1, \dots, X_{10}$  with increasing effect size. The red line indicates a CPI value of 0, corresponding to no estimated association between the variable  $X_j$  and the outcome  $Y$ . **B**: Histograms of simulation replications of  $t$ -statistics of variables with effect size 0. The distribution of the expected  $t$ -statistic under the null hypothesis is shown in red. **C**: Average proportion of rejected hypotheses at  $\alpha = 0.05$ . Results at effect size 0 correspond to the type I error, at effect sizes  $> 0$  to statistical power. The dashed line indicates the nominal level of  $\alpha = 0.05$ . The panels correspond to the simulation scenario, the colors and symbols to the learning algorithms and the line types to the inference procedure.

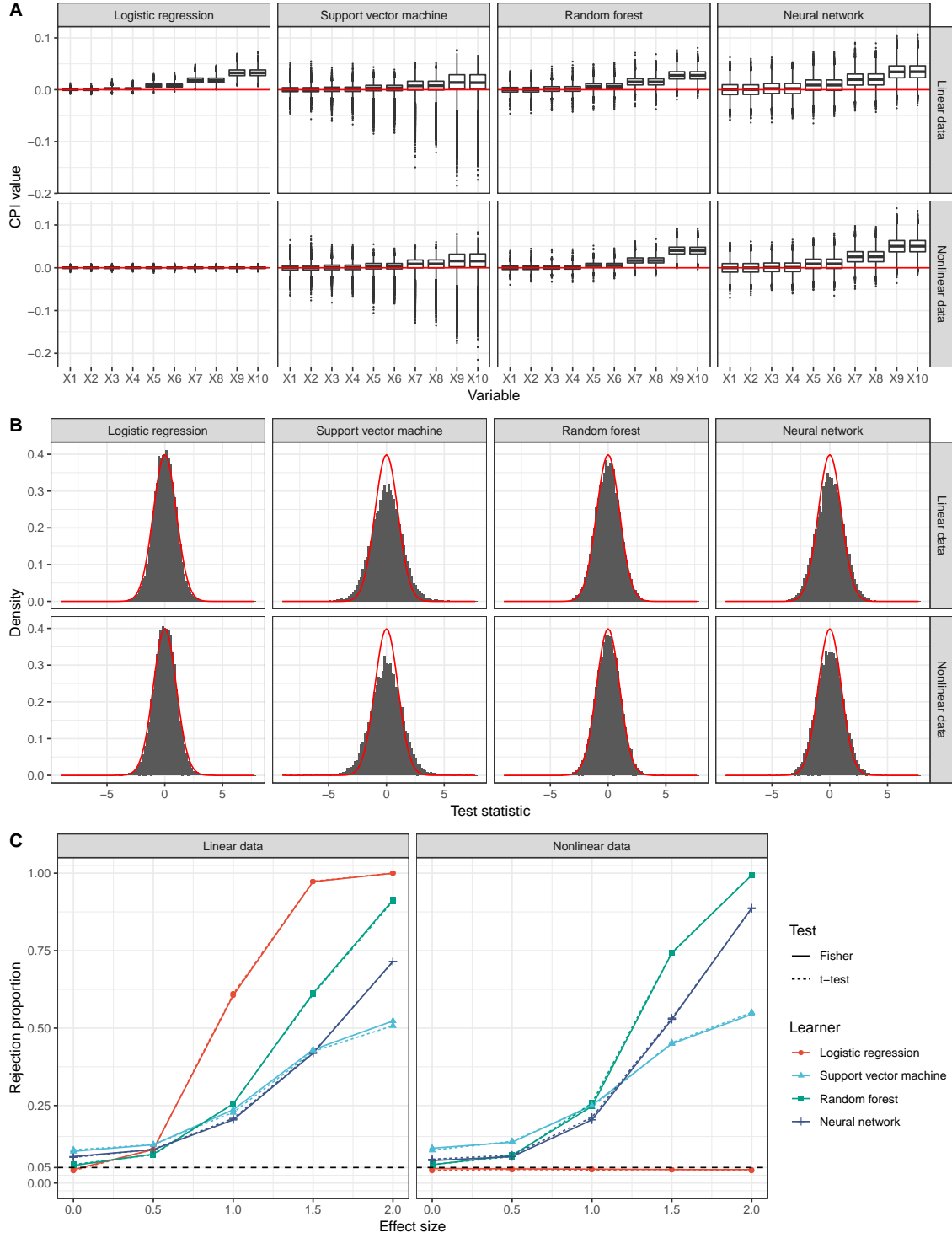


Figure S8: Simulation results for classification outcome with CE loss function and additive version of CPI. **A**: Boxplots of simulation replications of CPI values of variables  $X_1, \dots, X_{10}$  with increasing effect size. The red line indicates a CPI value of 0, corresponding to no estimated association between the variable  $X_j$  and the outcome  $Y$ . **B**: Histograms of simulation replications of  $t$ -statistics of variables with effect size 0. The distribution of the expected  $t$ -statistic under the null hypothesis is shown in red. **C**: Average proportion of rejected hypotheses at  $\alpha = 0.05$ . Results at effect size 0 correspond to the type I error, at effect sizes  $> 0$  to statistical power. The dashed line indicates the nominal level of  $\alpha = 0.05$ . The panels correspond to the simulation scenario, the colors and symbols to the learning algorithms and the line types to the inference procedure.

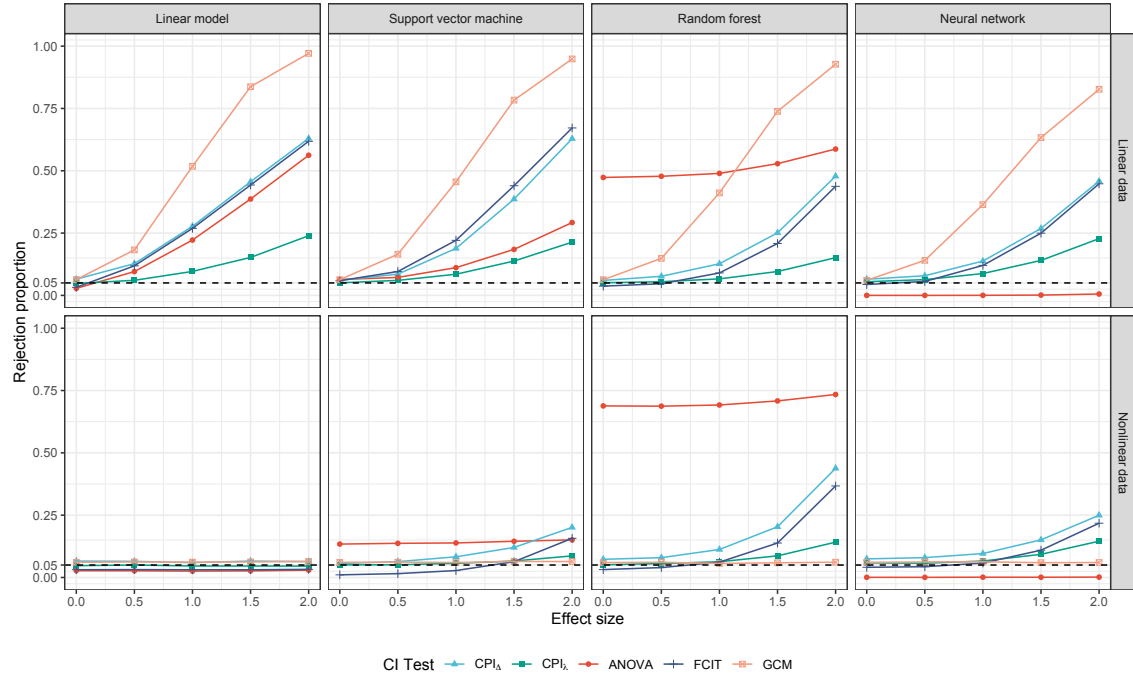


Figure S9: Comparative performance of VI measures across different simulations and algorithms, computed with a training sample of  $n = 100$  and a test sample of  $n = 50$ . Plots depict the proportion of rejected hypotheses at  $\alpha = 0.05$  as a function of effect size. Results at effect size 0 correspond to Type I error, at effect sizes  $> 0$  to statistical power. The dashed line indicates the nominal level of  $\alpha = 0.05$ .

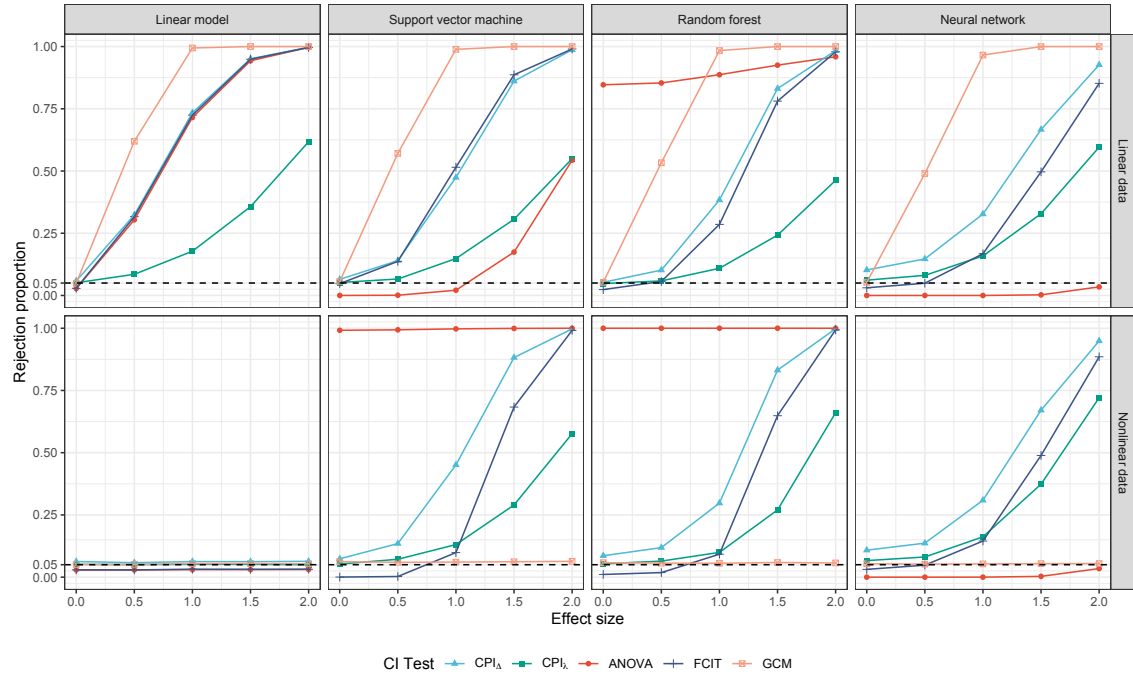


Figure S10: Comparative performance of VI measures across different simulations and algorithms, computed with a training sample of  $n = 500$  and a test sample of  $n = 250$ . Plots depict the proportion of rejected hypotheses at  $\alpha = 0.05$  as a function of effect size. Results at effect size 0 correspond to Type I error, at effect sizes  $> 0$  to statistical power. The dashed line indicates the nominal level of  $\alpha = 0.05$ .